



Naturalis Repository

Diversification of the phytophagous lineages of true bugs (Insecta:Hemiptera: Heteroptera) shortly after that of the flowering plants

Fei Ye, Petr Kment, David Redei, Jiu-Yang Luo, Yan-Hui Wang, Stefan M. Kuechler, Wei-Wei Zhang, Ping-Ping Chen, Hao-Yang Wu, Yan-Zhuo Wuh, Xiao-Ya Suni, Lu Ding, Yue-Ran Wang and Qiang Xie

DOI:

<https://doi.org/10.1111/cla.12501>

Downloaded from

[Naturalis Repository](#)

Article 25fa Dutch Copyright Act (DCA) - End User Rights


This publication is distributed under the terms of Article 25fa of the Dutch Copyright Act (Auteurswet) with consent from the author. Dutch law entitles the maker of a short scientific work funded either wholly or partially by Dutch public funds to make that work publicly available following a reasonable period after the work was first published, provided that reference is made to the source of the first publication of the work.

This publication is distributed under the Naturalis Biodiversity Center 'Taverne implementation' programme. In this programme, research output of Naturalis researchers and collection managers that complies with the legal requirements of Article 25fa of the Dutch Copyright Act is distributed online and free of barriers in the Naturalis institutional repository. Research output is distributed six months after its first online publication in the original published version and with proper attribution to the source of the original publication.

You are permitted to download and use the publication for personal purposes. All rights remain with the author(s) and copyrights owner(s) of this work. Any use of the publication other than authorized under this license or copyright law is prohibited.

If you believe that digital publication of certain material infringes any of your rights or (privacy) interests, please let the department of Collection Information know, stating your reasons. In case of a legitimate complaint, Collection Information will make the material inaccessible. Please contact us through email: collectie.informatie@naturalis.nl. We will contact you as soon as possible.

Diversification of the phytophagous lineages of true bugs (Insecta: Hemiptera: Heteroptera) shortly after that of the flowering plants

Fei Ye^{a,b}, Petr Kment^c, Dávid Rédei^d, Jiu-Yang Luo^{a,b}, Yan-Hui Wang^{a,b},
Stefan M. Kuechler^e, Wei-Wei Zhang^f, Ping-Ping Chen^g, Hao-Yang Wu^{a,b},
Yan-Zhuo Wu^h, Xiao-Ya Sunⁱ, Lu Ding^{a,b}, Yue-Ran Wang^{a,b} and Qiang Xie^{a,b*} 

^aState Key Laboratory of Biocontrol, Sun Yat-sen University, Guangzhou, China; ^bDepartment of Ecology and Evolution, School of Life Sciences, Sun Yat-sen University, Guangzhou, China; ^cDepartment of Entomology, National Museum, Praha, Czech Republic; ^dÓcsa, Hungary; ^eDepartment of Animal Ecology II, University of Bayreuth, Bayreuth, Germany; ^fThree Gorges Entomological Museum, Chongqing, China; ^gNetherlands Centre of Biodiversity Naturalis, Leiden, Netherlands; ^hTiangong University, Tianjin, China; ⁱTianjin Key Laboratory of Animal and Plant Resistance, Tianjin Normal University, Tianjin, China

Received 8 March 2021; Revised 20 February 2022; Accepted 22 February 2022

Abstract

More than 95% of phytophagous true bug (Hemiptera: Heteroptera) species belong to four superfamilies: Miroidea (Cimicomorpha), Pentatomoidea, Coreoidea, and Lygaeoidea (all Pentatomomorpha). These iconic groups of highly diverse, overwhelmingly phytophagous insects include several economically prominent agricultural and silvicultural pest species, though their evolutionary history has not yet been well resolved. In particular, superfamily- and family-level phylogenetic relationships of these four lineages have remained controversial, and the divergence times of some crucial nodes for phytophagous true bugs have hitherto been little known, which hampers a better understanding of the evolutionary processes and patterns of phytophagous insects. In the present study, we used 150 species and concatenated nuclear and mitochondrial protein-coding genes and rRNA genes to infer the phylogenetic relationships within the Terheteroptera (Cimicomorpha + Pentatomomorpha) and estimated their divergence times. Our results support the monophyly of Cimicomorpha, Pentatomomorpha, Miroidea, Pentatomoidea, Pyrrhocoroidea, Coreoidea, and Lygaeoidea. The phylogenetic relationships across phytophagous lineages are largely congruent at deep nodes across the analyses based on different datasets and tree-reconstructing methods with just a few exceptions. Estimated divergence times and ancestral state reconstructions for feeding habit indicate that phytophagous true bugs explosively radiated in the Early Cretaceous—shortly after the angiosperm radiation—with the subsequent diversification of the most speciose clades (Mirinae, Pentatomidae, Coreinae, and Rhyparochromidae) in the Late Cretaceous.

© 2022 Willi Hennig Society.

Introduction

True bugs (Hemiptera: Heteroptera), comprising more than 45 000 described extant species (Henry, 2017; Schuh & Weirauch, 2020), contain seven infraorders: Enicocephalomorpha, Dipsochoromorpha, Gerromorpha, Nepomorpha, Leptopodomorpha, Cimicomorpha, and Pentatomomorpha. Highly diverse, exclusively or predominantly phytophagous

clades belong to the latter two infraorders (Cimicomorpha and Pentatomomorpha, together comprising the Terheteroptera). Almost all phytophagous cimicomorphans belong to the Miroidea, of which the Thaumastocoridae and Tingidae feed exclusively on plants (Schaefer & Panizzi, 2000; Slater, 1973), while the Miridae are mostly phytophagous, with a minority being predatory or zoophytophagous (Wheeler, 2001). Apart from fungivorous Aradoidea, the other five pentatomomorphan superfamilies (Pentatomoidea, Idiositoloidea, Pyrrhocoroidea, Coreoidea, and Lygaeoidea, together comprising the Trichophora) are mainly

*Corresponding author:

E-mail address: xieq8@mail.sysu.edu.cn

phytophagous, with the exception of only a few lineages such as Asopinae (Pentatomoidea) and Geocorinae (Lygaeoidea; Schuh & Weirauch, 2020).

The vast majority of phytophagous true bugs belong to five superfamilies, Miroidea, Pentatomoidea, Lygaeoidea, Coreoidea, and Pyrrhocoroidea, the first four covering more than 95% of the species level diversity of this assemblage. Many species have considerable ecological and economic impact in natural environments and agricultural systems. Species of immense economic importance in their native distribution areas include *Lygus* and *Adelphocoris* spp. (Miridae), the primary pests of transgenic *Bacillus thuringiensis* cotton, causing serious quality and yield losses in Asia and North America (Layton, 2000; Lu et al., 2010; Wu et al., 2002), and the bean bug, *Riptortus pedestris* (Alydidae), one of the most destructive pests of soybean in Asia, significantly reducing yield by feeding on pods and seeds (Bae et al., 2014; Li et al., 2019b). Several phytophagous true bug species are invasive, the most well-known being the brown marmorated stink bug, *Halyomorpha halys* (Pentatomidae), a species native to Eastern Asia but introduced to North America and Europe where it inflicts severe damage upon many crops and horticultural plants (Hamilton et al., 2018; Leskey et al., 2012; Wermelinger et al., 2008).

Over the past several decades considerable effort has gone into clarifying terheteropteran phylogenetic relationships. The monophyly of both the infraorders Cimicomorpha and Pentatomomorpha as well as their sister relationship was supported by several studies (Cassis & Schuh, 2012; Johnson et al., 2018; de Moya et al., 2019; Schuh & Štys, 1991; Weirauch et al., 2019; Wheeler et al., 1993). Although the monophyly of most superfamilies and families included in these major clades is clear, there remain controversies on the relationships of specific higher taxa, such as superfamilial relationships within the Eutrichophora, i.e., alternative hypotheses: (i) Coreoidea + (Lygaeoidea + Pyrrhocoroidea), (ii) Lygaeoidea + (Coreoidea + Pyrrhocoroidea), and (iii) Pyrrhocoroidea + (Coreoidea + Lygaeoidea) (Henry, 1997; Hua et al., 2008; Li et al., 2016; Liu et al., 2019; Tian et al., 2011; Weirauch et al., 2019; Xie et al., 2005; Yuan et al., 2015).

Total-evidence phylogenetic analyses of Heteroptera based on a comprehensive sampling (Weirauch et al., 2019) provided to date the most robust phylogenetic framework for Cimicomorpha and Pentatomomorpha at superfamily level. Various detailed parts in the family- and subfamily-level phylogenetic relationships within the four major phytophagous superfamilies, however, still need to be further solved, especially for the early divergent groups of extant taxa for each superfamily, such as the position of Thaumastellidae within Pentatomoidea (Grazia et al., 2008; Lis et al., 2017; Weirauch et al., 2019; Wu et al., 2018), and

Isometopinae, Psallopinae and Cylapinae within Miridae (Jung & Lee, 2012; Namyatova & Cassis, 2019; Schuh et al., 2009; Schuh, 1974, 1976).

The evolution of feeding habits for true bugs has been studied recently, providing different evolutionary scenarios for the evolution of phytophagy within the group. Li et al. (2017) proposed that the phytophagy originated from the most recent common ancestor (MRCA) of Miridae and Pentatomomorpha based on the topology of non-monophyletic Cimicomorpha, while Weirauch et al. (2019) demonstrated a more reasonable evolutionary scenario that phytophagous Miroidea and Trichophora derived independently from predatory ancestors based on a widely supported monophyletic Cimicomorpha mentioned above. Such different evolutionary scenarios of phytophagy imply that a robust and correct phylogenetic relationship is the basis to evaluating the evolutionary patterns of feeding habits.

Divergence time estimations of Cimicomorpha and Pentatomomorpha have been reported, though most of them focused on deep nodes of Heteroptera and have poor samplings of phytophagous lineages. Divergence times inferred for various nodes within Cimicomorpha and Pentatomomorpha by previous studies appear to be imprecise. Notably, Miridae was inferred to diverge in the Permian or in the Cretaceous, with a huge variance of 184 Ma between the median estimated times (Johnson et al., 2018; Jung & Lee, 2012; Table 1). Meanwhile, little chronological discussion has been made focusing on the origin and diversification of phytophagous cimicomorphans and pentatomomorphans as a whole with comprehensive sampling of its diversity. Moreover, the potential driving forces including biotic and abiotic ecological factors for the diversification of phytophagous true bugs have not been comprehensively investigated, although the coevolution between plants and other phytophagous insects has been considered as an important factor for the diversification of phytophagous insects (Cruaud et al., 2012; Janz & Nylin, 1998; Janz et al., 2006; Percy et al., 2004).

In the present study we reconstruct the phylogeny of Terheteroptera (Cimicomorpha + Pentatomomorpha) based on concatenated 76 nuclear protein-coding genes (PCGs) selected from 98 taxa, and mitochondrial PCGs and rRNA genes of 150 taxa, covering all superfamilies within these two infraorders. Furthermore, we estimate divergence times to depict evolutionary timescales for Cimicomorpha and Pentatomomorpha based on the reconstructed phylogenetic trees reported here and multiple calibration points. Finally—combining the chronogram, the ancestral state reconstruction of feeding habit, and the currently recognized patterns of angiosperm evolution—we discuss the evolutionary timescale and possible driving forces for the diversification of phytophagous true bugs.

Table 1
Summary of estimated divergence times (Ma) for major groups of Tetheroptera from previous studies

Reference	Clade									
	Cimicomorpha	Miroidea	Miridae	Pentatomomorpha	Trichophora	Eutrichophora	Pentatomioidea	Lygacoidea	Corcoidea	
Johnson et al. (2018)	227	168	93	200	164	137	98	109	93	
Jung and Lee (2012)	–	–	277 (172–360)	–	–	–	–	–	–	
Li et al. (2012)	192	183	133	153	–	–	–	–	–	
Li et al. (2017)	–	195 (185–200)	137	212 (200–224)	198	181	128 (122–131)	165 (159–169)	157 (143–168)	
Liu et al. (2019)	–	–	–	237 (225–246)	217 (203–228)	181 (164–195)	165 (137–185)	142 (121–160)	162 (139–179)	
Wang et al. (2016)	216 (197–233)	163 (156–169)	–	211 (197–224)	193 (182–205)	180 (173–190)	144 (134–153)	167 (163–171)	161 (155–168)	
Wang et al. (2019)	210 (197–231)	163 (159–167)	–	207 (194–232)	191 (178–203)	176 (165–186)	142 (65–182)	132 (106–163)	–	

Materials and methods

Taxon sampling and generation of molecular data

A total of 150 terminal species were included in our taxon sampling, of which 42 cimicomorphans and 96 pentatomomorphans were ingroups, and three leptoDOMorphans and nine nepomorphans were used as outgroups. The 138 ingroup species represented 54 families, covering all 11 superfamilies and 90% of families in Terheteroptera. Among these, molecular data of 100 species were newly sequenced by Sanger sequencing or high-throughput-sequencing (HTS) in this study. For the Sanger method, total genomic DNA was extracted from legs or/and thorax of a single individual for 15 species, due to the limited availability of specimens, using DNeasy Blood and Tissue Kit (Qiagen); the remaining bodies were subsequently preserved in absolute ethanol as voucher specimens. Mitogenomes and complete 18S and 28S rDNA sequences were produced by PCR amplification employing universal primers (Table S1), Sanger sequencing, and fragments overlapping. The methods of PCR amplification and sequencing followed the description of Wang et al. (2016). For the HTS method, heads and thoraces were used to extract total genomic DNA using the CTAB method (Reineke et al., 1998). Independent DNA libraries for 85 species were built with an insert size of 250 base pairs (bp), and sequenced with a 150-bp paired end (PE) on the HiSeq X Ten platform at BGI Genomics (Shenzhen, China). Raw reads were pre-processed by removing reads containing adaptor contamination, poly-Ns (>5 bp Ns), and PE reads with >10 bases of low-quality scores (<20) (Wu et al., 2018). After data filtration, we obtained 10 073 914 to 30 823 226 clean reads per species. All the voucher specimens were deposited in the Systematic Entomology Lab, Sun Yat-sen University, Guangzhou, China. The rest of published mitogenomes, 18S and 28S rDNAs, genomes, and transcriptome data were downloaded from the National Center for Biotechnology Information database. The sampling list and the corresponding data accession numbers are provided in Table 2.

Assembly, annotation, and alignment

The Sanger sequencing data were assembled with Geneious software (Biomatters Ltd., Auckland, New Zealand), and the HTS data were *de novo* assembled using SOAPdenovo-Trans (Xie et al., 2014), followed by BLAST against local databases containing 18 known Heteroptera mitogenomes and 30 known complete Heteroptera 18S and 28S rDNAs, respectively, using the program BLAST+ (Camacho et al., 2009). All the reference sequences of mitogenomes and nrDNA were downloaded from the GenBank database.

Mitochondrial PCGs and 12S and 16S rDNAs were identified by alignment with homologous sequences through BLAST searches of GenBank. Boundary definitions of 18S and 28S rDNAs were also realized by alignment with homologous genes.

To better mine the HTS data for phylogenetic reconstruction, we used aTRAM 2.0 (Allen et al., 2018) to assemble extra nuclear PCG sequences from the HTS clean data. Firstly, aTRAM libraries of HTS clean data were built using the script *atram_preprocessor.py* available in the aTRAM package. The aTRAM assembly was run for three iterations using the Trinity (Grabherr et al., 2011) option for *de novo* assembly, with a reference set of 2394 single-copy orthologous PCG sequences from *Cimex lectularius* (<https://www.orthodb.org/>), which are also suggested to be single-copy orthologs in *Oncopeltus fasciatus*, *Gerris buenoi*, *Halyomorpha halys*, *Rhodnius prolixus*, *Myzus cerasi*, and *Homalodisca vitripennis*. All other parameters retained the default values. Next, the resulting contigs from aTRAM (BLAST values greater than 70) were processed using an exon stitching pipeline (https://github.com/juliema/exon_stitching) to

Table 2
Specimens used in this study and the corresponding NCBI accession numbers

Infraorder/Superfamily	Family	Subfamily	Species	HTS data	18S rDNA	28S rDNA	Mitogenome	
Cimicomorpha Cimicoidea	Anthocoridae	Cimicinae	<i>Orius insidiosus</i>	SRR1821945	GQ258415	GQ258450	KJ778890	
			<i>Cimex lectularius</i>	GCF_000648675	KJ461298	KJ461188	JQ739180	
			<i>Curallium cronini</i>	–	EU683128	–	–	
	Lycocoridae		<i>Lycotocoris beneficus</i>	–	EF487298	EF487324	EF487282, FJ917705 (<i>L. hasegawai</i>)	
				–	–	–	–	
	Microphysoidea	Plokiophilidae	Plokiophilinae	<i>Embiophila</i> sp.	–	MW633329*	MW629698*	MW619701*
				<i>Joppicus paradoxus</i>	–	AY252206	AY252455	EU683094
		Joppeidae		<i>Myrmedobia distinguenda</i>	–	MW633341*	MW629699*	MW619702*
				<i>Sophianus</i> sp.	–	MW633332*	MW629700*	MW619711-13*
		Microphysysidae	Miridae	<i>Deraeocoris</i> sp.	–	MW633334*	MW629701*	MW619700*
<i>Angerianus maurus</i>				–	MW633336*	MW629702*	MW619714-16*	
Miroidea		Psallopinidae		<i>Psallops</i> sp.	–	MW633335*	MW629703*	MW619708-10*
				<i>Xenocylapidius</i> sp.	–	MH179113	MH190438	MH156862, MH032592
		Cylapinae		<i>Amapacylapus</i> sp.	–	MH179118	MH190443	MH156866, MH032590
				<i>Adelphocoris lineolatus</i>	–	MH179102	MH190427	MH156851, MH016566
	Mirinae		<i>Onomaeus tenuis</i>	SRR6322463	KJ461200	KJ461163	KU234537	
			<i>Hyalolephus</i> sp.	SRR13843862*	MW629568*	MW629639*	MW619699*	
	Mirinae		<i>Mystilus priamus</i>	SRR13843851*	MW629571*	MW629640*	MW619698*	
			<i>Nesitocoris tenuis</i>	SRR13843840*	MW629570*	MW629638*	MW619697*	
	Bryocorinae		<i>Dicyphus</i> sp.	–	GU194646	GU194723	JQ806057	
			<i>Helopeltis</i> sp.	SRR13843829*	MW629569*	MW629637*	MW619696*	
Phyllinae		<i>Pilophorus typicus</i>	SRR13843818*	MW629567*	MW629636*	MW619695*		
		<i>Lasiolabops cosmopolites</i>	SRR13843812*	MW629566*	MW629635*	MW619694*		
Thaumastocoridae		<i>Mecomma ambulans</i>	–	MW633331*	MW629704*	MW619693*		
		<i>Cyrtorhinus</i> sp.	SRR13843894*	MW629565*	MW629705*	MW619692*		
Tingidae		<i>Thaumastocoris safordi</i>	–	KJ461271	KJ461187	MW619691*		
		<i>Onymocoris haekeri</i>	–	MW633328*	MW629706*	MW619690*		
Nabidae		<i>Cantacader</i> sp.	–	MW633330*	MW629707*	MW619689*		
		<i>Pseudacyta perseae</i>	–	KM278220	KM278221	KM278221		
Velocipedidae		<i>Corythucha ciliata</i>	SRR2051479	KJ461201	KJ461175	KC756280		
		<i>Metasalis populi</i>	–	KJ461270	KJ461246	MF351857		
Naboidea		<i>Haedus</i> sp.	SRR13843893*	MW629564*	MW629631*	MW619688*		
		<i>Alloeorhynchus</i> sp.	SRR13843873*	KJ461245	KJ461293	MW619687*		
Velocipedidae		<i>Nabis sinticus</i>	–	KJ461288	KJ461288	JF907590 (<i>N. apicalis</i>)		
		<i>Scotomedes</i> sp.1	SRR13843884*	–	–	JQ743677		
			<i>Scotomedes</i> sp.2	–	–	–	MW619728*	

(Continues)

Table 2
(Continued)

Infraorder/Superfamily	Family	Subfamily	Species	HTS data	18S rDNA	28S rDNA	Mitogenome			
Reduivoidea	Pachynomidae	Pachynominae	<i>Canarochilus</i> sp.	–	MF460825	MF460815	MF460805			
	Reduviidae	Holoptilinae	<i>Ptilocnemus lenur</i>	SRR13843896*	MW629560*	MW629630*	MW540749			
Pentatomomorpha	Aradoidea	Emesinae	<i>Ischnobanella hainana</i>	SRR13843895*	MW629563*	MW629629*	MW619686			
			<i>Brontostoma colossus</i>	–	KM278219	KM278219	KM044501			
		Triatominae	<i>Triatoma infestans</i>	SRR5765595	Y18750	GQ853396	KY640305	KY640305		
			<i>Chizocoris sinensis</i>	–	KJ461242	KJ461198	KC887532	KC887532		
		Coreoidea	Alydidae	Mezirinae	<i>Arbanatus</i> sp.	SRR13843886*	MW629577*	MW629641*	MW619704*	
					<i>Neuroctenus yunnanensis</i>	SRR13843885*	MW629579*	MW629643*	MW619726*	
				Mezirinae	<i>Neuroctenus</i> sp.	SRR13843883*	MW629580*	MW629644*	MW619719*	MW619685*
					<i>Mezira triangula</i>	–	MW633338*	MW629708*	MW619684*	MW619684*
				Alydinae	<i>Megalotomus</i> sp.	SRR13843882*	MW629578*	MW629642*	MW619718*	MW619684*
					<i>Riptortus pedestris</i>	SRR13843880*	MW629626*	MW629669*	MW619684*	EU427344
Micelytrinae	<i>Anacestra spiniger</i>			SRR13843879*	AB725684	MW629618*	MW629684*	MW619683*		
	<i>Grypocephalus pallipectus</i>			SRR13843881*	MW629620*	MW629687*	MW619682*	MW619682*		
Coreoidea	Coreidae			Coreinae	<i>Physomerus</i> sp.	SRR13843878*	MW629615*	MW629670*	MW619681*	
					<i>Notobitus elongatus</i>	SRR13843877*	MW629622*	MW629676*	MW619680*	
		Coreinae	<i>Hygia</i> sp.	SRR13843876*	MW629624*	MW629648*	MW619679*	MW619678*		
			<i>Enoplops sibiricus</i>	SRR13843875*	MW629619*	MW629681*	MW619677*	MW619677*		
		Coreinae	<i>Dalader distanti</i>	SRR13843874*	MW629608*	MW629677*	MW619676*	MW619676*		
			<i>Sinodasyneus</i> sp.	SRR13843872*	MW629621*	MW629680*	MW619725*	MW619725*		
		Coreinae	<i>Cletomorpha raja</i>	SRR13843871*	MW629609*	MW629675*	MW619675*	MW619675*		
			<i>Homocoeerus unipunctatus</i>	SRR13843870*	MW629627*	MW629678*	MW619724*	MW619724*		
		Coreinae	<i>Manocoeerus</i> sp.	SRR13843869*	MW629628*	MW629679*	MW619674*	MW619674*		
			<i>Helcomeria spinosa</i>	SRR13843868*	MW629613*	MW629682*	MW619673*	MW619673*		
Coreinae	<i>Petillopsis calcar</i>	SRR13843867*	MW629612*	MW629674*	MW619672*	MW619672*				
	<i>Hydarella orientalis</i>	SRR13843866*	MW629617*	MW629685*	MW619671*	MW619671*				
Pseudophloeinae	Hyocephalidae	<i>Grallilava horrens</i>	SRR13843865*	MW629625*	MW629686*	AY252957, AY252692				
		<i>Maevius indecorus</i>	–	AY252214	AY252463	MW619670*				
Rhopalidae	Rhopalinae	<i>Chorosoma</i> sp.	SRR13843864*	MW629614*	MW629672*	MW619669*				
		<i>Rhopalus maculatus</i>	SRR13843863*	MW629616*	MW629673*	MW619668*				
Stenocephalidae	Stenocephalidae	Serinethinae	<i>Leptocoris augur</i>	SRR13843861*	MW629611*	MW629671*	MW619667*			
			<i>Dicranocephalus alticolus</i>	SRR13843860*	KJ461228	KJ461267	MW619666*			
		<i>Dicranocephalus</i> sp.	SRR13843859*	MW629623*	MW629683*	MW619666*	AY252961, EU683093			
		<i>Henicocoris monteithi</i>	–	AY252218	EU683199	AY252961, EU683093				
Idiostoloidea	Idiostolidae	<i>Idiostolus</i> sp.	–	MW633337*	MW629709*	MW619707*				

(Continues)

Table 2
(Continued)

Infraorder/Superfamily	Family	Subfamily	Species	HTS data	18S rDNA	28S rDNA	Mitogenome	
Lygaeoidea	Artheneidae	Artheneinae	<i>Artheneis intricata</i>	SRR13843845*	KJ461299	KJ461203	MW619665*	
	Blissidae		<i>Cavelerius excavatus</i>	SRR13843844*	KJ461294	KJ461237	MW619664*	
Berytidae	Metacanthinae		<i>Macropus robustus</i>	SRR13843843*	MW629587*	MW629647*	MW619663*	
			<i>Metacanthus pulchellus</i>	SRR13843842*	MW629572*	MW629654*	MW619662*	
	Colobathristidae		<i>Metatropis brevisrostris</i>	SRR13843841*	MW629573*	MW629653*	MW619661*	
			<i>Phaenacantha marcida</i>	SRR13843839*	MW629602*	MW629694*	MW619660*	
	Cryptorhamphidae		<i>Cryptorhamphus</i> sp.	SRR13843821*	MW629606*	MW629655*	MW619659*	
			<i>Cymus</i> sp.	SRR13843838*	MW629575*	MW629656*	MW619658*	
	Cymidae	Geocorinae	<i>Geocoris pallidipennis</i>	SRR13843837*	MW629588*	MW629691*	MW619657*	
		Henestarinae	<i>Henestaris halophilus</i>	SRR13843836*	MW629597*	MW629690*	MW619656*	
	Heterogastridae			<i>Sadoletus valdezi</i>	SRR13843835*	MW629603*	MW629660*	MW619655*
				<i>Dinomaachus sikhimensis</i>	SRR13843819*	MW629604*	MW629658*	MW619654*
		<i>Parathyginus</i> sp.	SRR13843817*	MW629605*	MW629659*	MW619653*		
Lygaeidae		Lygaeinae	<i>Arocatus melanocephalus</i>	SRR13843834*	MW629607*	MW629677*	MW619723*	
		Ischnorhynchinae	<i>Crompus oculatus</i>	SRR13843833*	MW629589*	MW629689*	MW619652*	
Malcidae		Orsillinae	<i>Nithecus jacobaeae</i>	SRR13843832*	MW629587*	MW629696*	MW619651*	
		Malcinae	<i>Malcus auriculatus</i>	SRR13843831*	MW629591*	MW629692*	MW619722*	
			<i>Malcus setosus</i>	SRR13843830*	MW629592*	MW629693*	MW619717*	
Meschiidae			<i>Meschia woodwardi</i>	SRR13843820*	MW629596*	MW629651*	MW619650*	
		Nimidae	<i>Ninus insignis</i>	SRR13843828*	MW629576*	MW629657*	MW619729*	
Oxyarenidae		<i>Oxyarenus lugubris</i>	SRR13843827*	MW629594*	MW629662*	MW619706*		
	Piesmatidae	<i>Piesma cf. maculatum</i>	SRR13843826*	MW629574*	MW629645*	MW619649*		
Pachygronthidae	Pachygronthinae		<i>Pachyphlegyas modigliani</i>	SRR13843825*	MW629586*	MW629664*	MW619648*	
			<i>Opisholeptus burmanus</i>	SRR13843816*	MW629598*	MW629663*	MW619647*	
	Teracrinae		<i>Stenophylla maereta</i>	SRR13843815*	MW629595*	MW629661*	MW619646*	
			<i>Harmostica fulvicornis</i>	SRR13843824*	MW629590*	MW629655*	MW619721*	
	Rhyparochromidae		<i>Bryanellocoris orientalis</i>	SRR13843823*	MW629601*	MW629688*	MW619720*	
			<i>Appolonius erassus</i>	SRR13843822*	MW629593*	MW629652*	MW619645*	
	Physopeltinae		<i>Macroheraia grandis</i>	SRR13843892*	MW629583*	MW629665*	KX355212	
			<i>Physopelta quadriguttata</i>	SRR13843891*	MW629584*	MW629666*	MW619644*	
	Largidae		<i>Largus</i> sp.	SRR13843890*	MW629610*	MW629668*	MW619643*	
			<i>Physopelta</i> sp.	SRR13843889*	MW629585*	MW629667*	MW619642*	
Pyrrhocoridae		<i>Dysdercus cingulatus</i>	SRR5040256	KJ461263	KJ461235	EU427335		
		<i>Pyrrhocoris apterus</i>	SRR2051509	KX821833	KX821848	KX355214 (<i>P. sibiricus</i>)		
Pentatomidea			<i>Myrmoplasta mira</i>	–	MW633340*	MW629710*	MK809516	
			<i>Ectatops</i> sp.	–	MW629600*	MW629649*	MW619641*	
	Acanthosomatidae		<i>Scantius aegyptius rossii</i>	–	MW633339*	MW629711*	MW619640*	
			<i>Dysdercus evanescens</i>	SRR13843887*	MW629599*	MW629650*	MW619727*	
		<i>Acanthosoma nigrodorsum</i>	SRR13843858*	KJ522637	KJ522637	MF162952, MF162995, MF173617, MF173660, MF173703, MF173789, MF173832, MF173875, MF173918, MF173961, MF174004, MF078012, LC099119, LC099172		
		<i>Sastragala edessoides</i>	–	KJ535882 (<i>Sastragala</i> sp.)	KJ535882 (<i>Sastragala</i> sp.)	KJ535882 (<i>Sastragala</i> sp.)	JQ743676	

(Continues)

Table 2
(Continued)

Infraorder/Superfamily	Family	Subfamily	Species	HTS data	18S rDNA	28S rDNA	Mitogenome
Canopidae Cydnidae	Cydninae Cydninae		<i>Canopus</i> sp.	–	AY252229	AY22472	AY252969, AY252700
			<i>Macroscytus fraterculus</i>	–	KJ535876	KJ535876	EU427338 (<i>M. gibbultus</i>)
			<i>Microporus nigrita</i>	SRR13843857*	KJ535880	KJ535880	MF162975, MF163018, MF173640, MF173683, MF173726, MF173769, MF173812, MF173855, MF173898, MF173941, MF173984, MF174027, MF078035, JQ029117, JQ029137
Dinidoridae	Dinidorinae	<i>Cyclopelta parva</i>	–	KJ522641 (<i>C. obscura</i>)	KJ522642 (<i>C. obscura</i>)	KY069962	
		<i>Megymenium</i> sp.	SRR13843856*	KJ535879	KJ535879	MF162974, MF163017, MF173639, MF173682, MF173725, MF173768, MF173811, MF173854, MF173897, MF173940, MF173983, MF174026, MF078034, AY252697	
Lestoniidae Megaridiidae Parastrachidae		<i>Lestonia haustorifera</i>	–	KT188471	KT188472	AY252925, AY252664	
		<i>Megarid</i> sp.	SRR13843855*	MW629581*	MW629646*	MW619639*	
		<i>Parastrachia japonensis</i>	–	EF641204	EF641184	JQ029116, EF641132, EF641158 MG182695	
Pentatomidae	Phyllocephalinae	<i>Gonopsis affinis</i>	–	KJ535872 (<i>Gonopsis</i> sp.)	KJ535872 (<i>Gonopsis</i> sp.)	MF805778	
		<i>Picromerus griseus</i>	–	KJ535896 (<i>P. lewisi</i>)	KJ535891 (<i>P. lewisi</i>)		
Plataspidae	Podopinae	<i>Erthesina fullo</i>	SRR1611129	KJ535866	KJ535866	JQ743673	
		<i>Graphosoma rubrolineatum</i>	–	KT188469 (<i>G. lineatum</i>)	KT188470 (<i>G. lineatum</i>)	KX267740	
		<i>Brachyplatys subaeneus</i>	SRR13843854*	KY495690	KY495723	KT447151, MF078016, MF174008, MF173965, MF173922, MF173879, MF173836, MF173793, MF173750, MF173707, MF173664, MF173621, MF162999, MF162956 EU427334	
Saileriolidae		<i>Coptosoma bifarium</i>	–	KJ461259	KJ461239	EU427334	
		<i>Bannacortis arboreus</i>	SRR13843846*	KT188467	KT188468	MF078015, MF162955, MF162998, MF173620, MF173663, MF173706, MF173749, MF173792, MF173835, MF173878, MF173921, MF174007, MF173964	

(Continues)

Table 2
(Continued)

Infraorder/Superfamily	Family	Subfamily	Species	HTS data	18S rDNA	28S rDNA	Mitogenome									
Scutelleridae	Elvisurinae	<i>Solenosthedium bilunatum</i>		SRR13843853*	KY495658	KY495691	MF162986, MF163029, MF173651, MF173694, MF173737, MF173780, MF173823, MF173866, MF173909, MF173952, MF173995, MF174038, MF078046 MF162972, MF163015, MF173637, MF173680, MF173723, MF173766, MF173809, MF173852, MF173895, MF173938, MF173981, MF174024, MF078032 MF162980, MF163023, MF173645, MF173688, MF173731, MF173774, MF173817, MF173860, MF173903, MF173946, MF173989, MF174032, MF078040 MF162971, MF163014, MF173636, MF173679, MF173722, MF173765, MF173808, MF173851, MF173894, MF173937, MF173980, MF174023, MF078031 MF162962, MF163005, MF173627, MF173670, MF173713, MF173756, MF173799, MF173842, MF173885, MF173928, MF173971, MF174014, MF078022 JQ910983 EF641176, EF641148 EF641147, EF641175 JQ743678									
							Odontoscelinae	<i>Irochrotus sibiricus</i>	SRR13843852*	KY495660	KY495693	MF162993, MF163036, MF173658, MF173701, MF173744, MF173787, MF173830, MF173873, MF173916, MF173959, MF174002, MF174045, MF078053				
												Pachycorinae	<i>Orsilochides guttata</i>	SRR13843850*	KY495672	KY495705
							Tessaratominae	<i>Dalcantha cf. alata</i>	SRR13843848*	KJ535862	KJ535862					
												Tessaratominae	<i>Eusthenes cupreus</i>	KJ535869	KJ535869	
																Tessaratominae
							Tessaratominae	<i>Thaumastella elizabethae</i>	EF641221	EF641195						
											Tessaratominae	<i>Urochela quadrinotata</i>	KJ535884	KJ535884		
															Tessaratominae	<i>Urolabida menghaiensis</i>
							Thaumastellidae	<i>Urolabida menghaiensis</i>	SRR13843847*	KJ535885						
											Urostylididae	<i>Urolabida menghaiensis</i>	SRR13843847*	KJ535885		

(Continues)

Table 2
(Continued)

Infraorder/Superfamily	Family	Subfamily	Species	HTS data	18S rDNA	28S rDNA	Mitogenome
Leptopodomorpha Leptopodoidea	Leptopodidae Saltidae	Leptopodinae Saltinae	<i>Urostylis flavoannulata</i>	–	KJ535886 (<i>U. chinai</i>)	KJ535886 (<i>U. chinai</i>)	KY069970
			<i>Valleriotea javanica</i>	SRR13843813*	MW629562*	MW629632*	MW619638*
			<i>Saldula arsenjevi</i>	SRR2051510 (<i>S. saltatoria</i>)	KJ461170 (<i>S. saltatoria</i>)	KJ461213 (<i>S. saltatoria</i>)	EU427345
Nepomorpha Corixoidea	Corixidae	Corixinae	<i>Calacanthia angulosa</i>	SRR13843814*	MW629561*	MW629633*	MW619703*
			<i>Sigara septemlineata</i>	–	FJ372642 (<i>Sigara</i> sp.)	FJ372661 (<i>Sigara</i> sp.)	FJ456941
Naucoroidea	Corixidae	Micronectinae	<i>Micronecta sahbergii</i>	–	AY252216 (<i>Micronecta</i> sp.)	AY252465 (<i>Micronecta</i> sp.)	MH382835
			<i>Aphelocheirus ellipsoideus</i>	SRR2051467 (<i>A. aestivalis</i>)	KJ461184	KJ461297	FJ456939
			<i>Diplonychus rusticus</i>	SRR2051483	KJ461227	KJ461265	FJ456940
			<i>Helotrephes semiglobosus</i>	–	KJ461195	KJ461215	KJ027513
Ochteroidea	Pleidae	Nerthrinae	<i>Enithares tibialis</i>	SRR5137134 (<i>E. bimpressa</i>)	KJ461179 (<i>E. chinensis</i>)	KJ461179 (<i>E. chinensis</i>)	FJ456949
			<i>Paraplea frontalis</i>	–	KJ461252	KJ461196	KJ027516
			<i>Nerthra indica</i>	SRR5040129	KJ461313	KJ461276	FJ456943
	Ochteridae		<i>Ochterus marginatus</i>	–	KJ461251	KJ461315	FJ456950

* Indicates newly sequenced data in this study.

identify and stitch together the exons of each gene. Afterwards, for further sifting the best matching contigs, we used Orthograph (Peteresen et al., 2017) to map all contigs for each species to a set of target orthologous genes, which were built using the single copy genes mentioned above. Finally, the accompanying script *summarize_orthograph_results.pl* was used to summarize the Orthograph results from all taxa. All Orthograph parameters were left at the default values.

After batch filtering the primary nuclear orthologous genes, retaining only genes present in more than 74 species, all the nuclear and mitochondrial PCGs were aligned individually using Multiple Alignment using Fast Fourier Transform (MAFFT) software with the L-INS-i algorithm (Katoh & Standley, 2013) at the translational (amino acid) level. The alignments of corresponding nucleotide sequences were conducted using a local version of TranslatorX (Abascal et al., 2010). Simultaneously, ambiguously aligned sites were removed from both the amino acid and the nucleotide alignments using GBlocks (-b3 = 8, -b4 = 5, -b5 = h options) implemented in TranslatorX. Then, we further filtered the genes by removing sequences composed mainly of gaps or alignments shorter than 33 amino acids. We also implemented a batch filtering to remove sequences composed mainly of “X” and “NNN” at amino acid and nucleotide level, respectively. Genes with fewer than 75 taxa (50% of total sampling) were waived. Therefore, 76 PCGs were retained for the following analyses. Four RNA genes were individually aligned with MAFFT using the L-INS-i algorithm, and the original alignments were checked and manually corrected on the basis of the secondary structure models (Li et al., 2013; Yu et al., 2013). Subsequently, the ambiguous regions were deleted using GBlocks with the same parameters.

PCGs and RNA genes were concatenated to two matrices, namely PCGAARNA and PCGNT12RNA (Dataset S1 and S2). The former matrix comprised nucleotide sequences of four RNA genes and amino acid sequences of the 89 PCGs with a total of 6651 nucleotide sites and 21 977 aligned amino acid sites, respectively. The latter matrix showed 50 605 aligned nucleotide sites in length, including four RNA genes and only the first two codon positions of the 89 PCGs. Using the saturation analysis provided by DAMBE 5 (Xia, 2013), the substitution of the third codon position of the PCGs was detected as saturated (Table S2), and thus the nucleotides in the third codon positions were excluded from the matrix.

Phylogenetic inference and divergence time estimation

Phylogenetic analyses were performed using maximum likelihood (ML), Bayesian inference (BI), and parsimony methods based on the two matrices. IQ-TREE (Nguyen et al., 2015) was used to examine substitution models and partitioning schemes of two supermatrices under the corrected Akaike information criterion with the default model set of ModelFinder (Kalyaanamoorthy et al., 2017) for ML analyses, and the Bayesian information criterion with Bayesian model set for BI analyses respectively. The ML analyses were also conducted using IQ-TREE with the estimated best-fit model assigned to each of 46 and 66 partitions for PCGAARNA and PCGNT12RNA datasets, respectively (Table S3). Nodal support values were inferred using the ultrafast bootstrap approach with 5000 replicates (Hoang et al., 2018). Bayesian inferences were implemented by the MPI version of MrBayes 3.2.6 (Ronquist et al., 2012) with the appropriate models for 25 and 28 partitions with regard to the PCGAARNA and PCGNT12RNA data sets (Table S3). Two simultaneous runs with each of four Markov chains (three heated and one cold) were conducted with a random starting tree for 20 000 000 generations and sampled every 1000 generations. Convergence was confirmed by visualized likelihood values against the generation number, and the first 1 000 000 generations were discarded as burn-in. For parsimony analyses executed in TNT (Goloboff & Catalano, 2016), the tree searches were run by new technology

search method with rigorous parameter settings (initial level 99 and hits 20) and sectorial search, ratchet, drift, and tree fusing options. The nepomorphan species *Sigara septemlineata* was used as the outgroup for parsimony analyses of TNT. One and ten parsimony trees were found for PCGNT12RNA and PCGAARNA datasets, respectively, and then a majority-rule consensus tree with a cut off of 50% was calculated from the ten parsimony trees of PCGAARNA dataset. All characters shared equal weighting and gaps were regarded as missing characters. Clade robustness was assessed by 1000 replicates of standard bootstrap resampling with collapsing rule 1. Apart from the aforesaid phylogenetic analyses based on two 150-species matrices, to test the effect of outgroup sampling additional ML analyses using the same parameter settings were performed based on another two matrices which excluded all sequences of nine nepomorphans.

MCMCTree from the Phylogenetic Analysis by Maximum Likelihood (PAML) 4.9 package (Yang, 2007) was used to estimate divergence times of Cimicomorpha and Pentatomomorpha with a relaxed molecular clock based on all six topologies corresponding to the datasets PCGNT12RNA and PCGAARNA, and 16 nodes were calibrated with fossil records. According to the assessed overall mutation rate (0.078270 per unit time for PCGNT12RNA dataset; 0.081255 per unit time for PCGAARNA dataset) obtained utilizing baseml (in PAML) under the GTR+G substitution model (model = 7, alpha = 0.5) and codeml (in PAML) under empirical substitution model (model = 2, alpha = 0.5), the Dirichlet-gamma prior for the overall substitution rate was set as *rgene_gamma* = 1, 13 for PCGNT12RNA dataset and *rgene_gamma* = 1, 12 for PCGAARNA dataset. The MCMCTree program was run for 2 500 000 MCMC steps and sampled every 50 after a 50 000 burn-in. The robustness of the MCMCTree results was checked by comparing the consistency of at least two independent runs, with all parameters at least 200 for the effective sample sizes. The lineage-through-time (LTT) plots were generated using the R package *phytools* with the *ltt* function (Revell, 2012) at the subfamily level—based on the pruned chronogram (one individual per subfamily) of six trees inferred from both PCGNT12RNA and PCGAARNA datasets in this study—for true bugs, and at the order level—based on the reported chronogram of seed plants (Li et al., 2019a)—for angiosperms. The pruning of six trees of true bugs was conducted using the *ape* package with the *drop.tip* function (Paradis & Schliep, 2019). The six LTT plots of true bugs were drawn using the pruned chronogram of phytophagous lineages. In addition, the reported chronogram of seed plants only contains two gymnosperm splits during the past 250 Ma; therefore, the range of LTT from 250 Ma to present can represent the angiosperm evolutionary history.

As for the demonstration of the used fossils, the details for 16 nodes are summarized in Table 3. Most nodes used the oldest fossil records for corresponding taxonomic categories, with a few exceptions, e.g., Tingidae node (Appendix S1). The earliest fossil of Tingidae in the Paleobiology Database (<https://paleobiology.org/>) is *Archetingis ladinnica*, dated back to 242.0–235.0 Ma, but that fossil is considered as a doubtful taxonomic placement (Schuh & Weirauch, 2020), as well as our opinion; a boom in tingid fossils began only in the lower Cretaceous Aptian Stage (125.0–113.0 Ma). To reduce the risk of potentially erroneous placement of the oldest fossil record, we selected the second oldest fossil record, *Golmonia pater* (125.0–113.0 Ma), to calibrate the Tingidae node. Apart from the calibrating nodes of the root, Nepomorpha, and Leptopodomorpha, all the rest of calibrating nodes used an additional earlier Stage/Age and an additional later Stage/Age based on the Stage/Age of the fossil species belonging to set the starting and the ending time of soft boundaries with 95% confidence interval.

Ancestral character state reconstruction

To explore the evolution of phytophagy in true bugs, we built a dataset of feeding habits following a careful survey to conduct

Table 3
Fossil calibrations used in divergence time estimation

Calibration node	Fossil record	Taxonomic group	PBDB age (Ma)	Prior distributions and shapes	References
Root	<i>Actinoscytina belmontensis</i>	Coleorrhyncha: Progonocimicidae	254.17–252.17	B (2.472,2.541,0.025,0.025)	Tillyard (1926)
	<i>Arlecoris louisi</i>	Naucoroidea: Triassocoridae	247.2–242.0		Shcherbakov (2010)
Nepomorpha	<i>Arlecoris louisi</i>	Naucoroidea: Triassocoridae	247.2–242.0	B (2.28,2.472,0.025,0.025)	Shcherbakov (2010)
	<i>Lufengnacta corrugis</i>	Corixoidea	228.0–208.5		Lin (1977)
Ochtheroidea + (Naucoroidea+ Notonectoidea)	<i>Propreocoris maculatus</i>	Ochtheroidea: Propreocoridae	196.5–189.6	B (1.827,2.013,0.025,0.025)	Popov et al. (1994)
Notonectoidea	<i>Liadonecta tomiensis</i>	Notonectoidea: Notonectidae	182.7–170.3	B (1.683,1.908,0.025,0.025)	Popov (1971)
Leptopodomorpha	<i>Britannicola senilis</i>	Saldoidea: Archegocimicidae	208.5–201.3	B (1.82,2.085,0.025,0.025)	Popov et al. (1994)
	multiple	Leptopodomorpha	183.0–182.0		
Naboidea	<i>Karanabis kiritshenkoi</i>	Naboidea: Nabidae	166.1–157.3	B (1.521,1.683,0.025,0.025)	Becker-Migdisova (1962)
Tingidae	<i>Golmonia pater</i>	Miroidea: Tingidae: Cantacaderinae: Golmoniini	125.0–113.0	B (1.005,1.294,0.025,0.025)	Popov (1989)
Isometopinae	<i>Myiomma voigti</i>	Miroidea: Miridae: Isometopinae: Myiommini	38.0–33.9	B (0.2782,0.412,0.025,0.025)	Popov and Herczek (1992)
Mirinae	<i>Cretamystilus herczeki</i>	Miroidea: Miridae: Mirinae: Mecistoscelini	99.6–93.5	B (0.898,1.13,0.025,0.025)	Kim and Jung (2021)
Mezirinae	<i>Myanmezira longicornis</i>	Aradoidea: Aradidae: Mezirinae	99.6–93.5	B (0.898,1.13,0.025,0.025)	Heiss and Poinar (2012)
Urostylididae	<i>Urochela pardalina</i>	Pentatomoidea: Urostylididae: Urostylidinae: Urostylidini	20.44–15.97	B (0.1382,0.2303,0.025,0.025)	Zhang (1989)
Cydnidae + (Dinidoridae + Tessaratomidae)	<i>Cilicydnus robustispinus</i>	Pentatomoidea: Cydnidae: Amnestinae	125.45–122.46	B (1.13,1.294,0.025,0.025)	Yao et al. (2007)
Dinidoridae	<i>Dinidorites margiformis</i>	Pentatomoidea: Dinidoridae	56.0–47.8	B (0.412,0.592,0.025,0.025)	Cockerell (1921)
Acanthosomatidae	<i>Acanthosoma</i> sp.	Pentatomoidea: Acanthosomatidae	15.97–11.608	B (0.072,0.2044,0.025,0.025)	Fujiyama (1987)
Micrelytrinae	<i>Eothes elegans</i>	Coreoidea: Alydidae: Micrelytrinae	37.2–33.9	B (0.2782,0.412,0.025,0.025)	Swanson (2020)
Berytidae	<i>Metacanthus serratus</i>	Lygaeoidea: Berytidae	33.9–28.4	B (0.2303,0.3771,0.025,0.025)	Theobald (1937)

ancestral character reconstructions using the ML method implemented in MESQUITE 3.61 (Maddison & Maddison, 2019). The Markov *k*-state 1 parameter model was used in the ML ancestral character reconstruction. Feeding habits were analyzed with the following defined types: fungivorous, predatory (including hematophagous and scavenging), phytophagous sap-feeding, phytophagous seed-feeding and phytophagous mesophyll-feeding (Table S4).

Results

Phylogenetic analyses

The results of ML analyses inferred from PCGNR12RNA dataset and summarized support

values of BI and parsimony analyses are shown in Fig. 1, and the specific topologies for these analyses are presented in Figs S1–S8. The monophyly of Cimicomorpha and Pentatomomorpha was confirmed in all analyses, and the sister group relationship between them was recovered with strong support values. Nearly all the superfamilies were consistently recovered as monophyletic. Within Cimicomorpha, Reduvidae was recovered as the sister group of the remaining cimicomorphans, and Miroidea was grouped with Cimiciformes *sensu lato* comprising Microphysoidea, Nabidae, and Cimicoidea. Within Pentatomomorpha, analyses consistently supported the Aradoidea as the sister group to the remaining lineages. For the

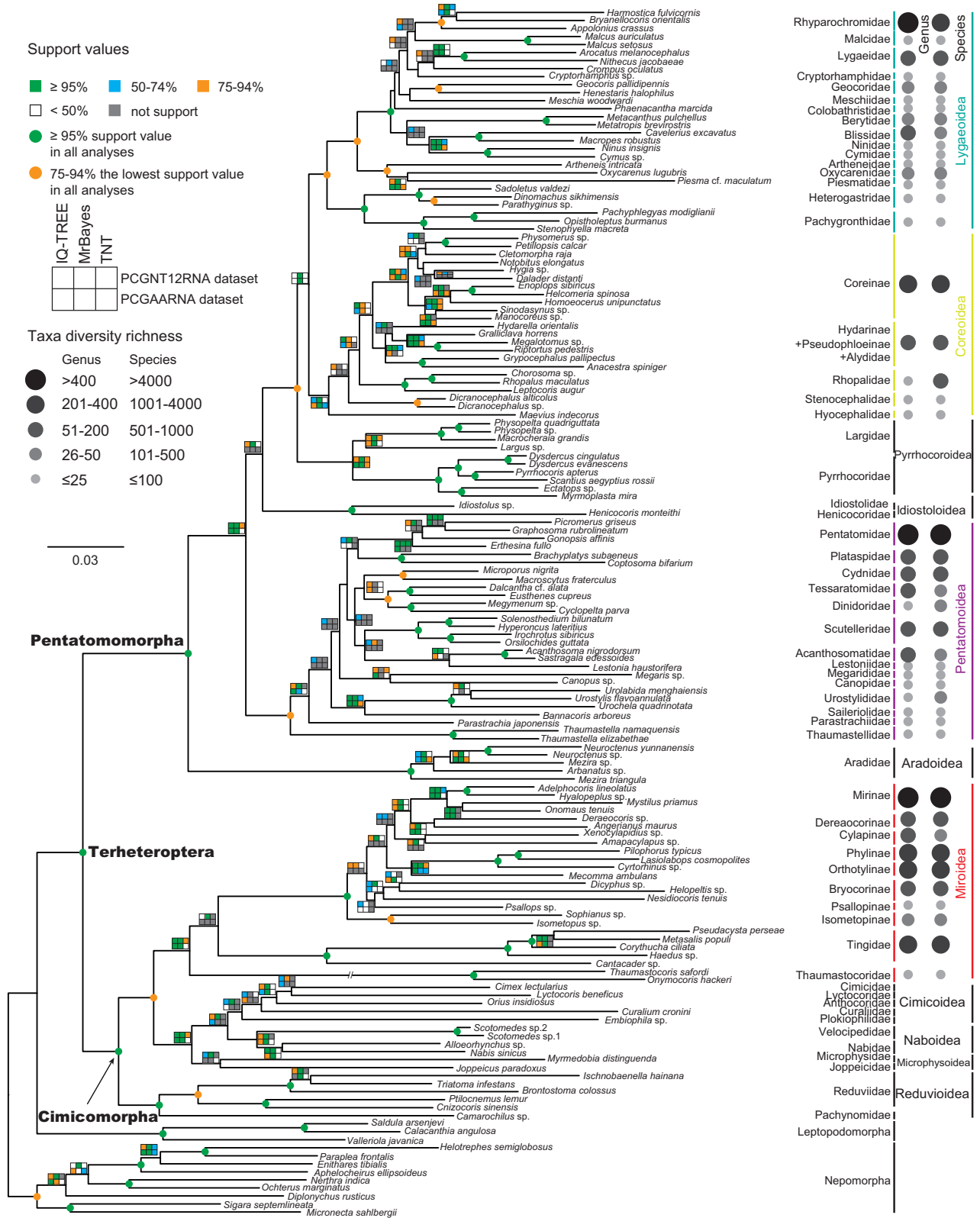


Fig. 1. Phylogenetic tree of Terheteroptera inferred from maximum-likelihood analyses based on PCGNT12RNA dataset covering 150 taxon samples. The bootstrap values of maximum-likelihood analyses and parsimony analyses, and posterior probabilities of Bayesian analyses are summarized and labelled around each node. Gray balls on the right indicate the taxa diversity richness of each family or subfamily within four major phytophagous superfamilies (Henry, 2017; Schuh & Weirauch, 2020).

phylogenetic relationships among the superfamilies of Trichophora, the results of PCGNT12RNA dataset repeatedly recovered the framework as Pentatomoidea + (Idiostoloidea + (Pyrrhocoroidea + (Coreoidea + Lygaeoidea))).

Within Miroidea, all families were recovered as monophyletic. Within Miridae, Isometopinae was placed as the sister group to the remaining mirids in phylogenetic trees of PCGNT12RNA dataset. Orthotylinae was grouped with Phylinae in all analyses, and Mirinae was recovered as the sister group to Deraeocorinae in most analyses.

Within Pentatomoidea, Thaumastellidae was recognized as the sister group to the remaining pentatomoids. Although the topologies within Pentatomoidea were not stable, the sister group relationships between Lestoniidae and Acanthosomatidae as well as Cydnidae *sensu stricto* (*sensu* Pluot-Sigwalt & Lis, 2008) and (Dinidoridae + Tessaratomidae) were consistently supported in most topologies. In addition, Pentatomidae was recovered as the sister group to Plataspidae in most topologies. The hypothesis of Cydnidae *sensu lato* (*sensu* Dolling, 1981; see also Schuh & Weirauch, 2020) was rejected.

Within Coreoidea, Hyocephalidae, and Stenocephalidae were the early divergent lineages of extant coreoids, and Rhopalidae was recovered as the sister group to Coreidae and Alydidae. All analyses strongly suggested the non-monophyly of both Coreidae and Alydidae, since both the coreid subfamilies Hydarinae and Pseudophloeinae were nested within Alydidae, which further clustered with Coreinae as the sister group.

Within Lygaeoidea, all analyses strongly suggested an early split of a lineage comprising Pachygronthidae and Heterogastridae, which was recovered as the sister group to the rest of the lygaeoid lineages. Two additional well-supported groups, namely Artheneidae + (Oxycarenidae + Piesmatidae) and Blissidae + (Ninidae + Cymidae), were also constant in topologies. Rhyparochromidae and Malcidae were allied together as a monophyletic group in ML analyses. The phylogenetic reconstructions based on matrices including or excluding nepomorphan data showed almost identical topologies, with only a few differences (Figs S9 and S10).

Divergence time estimation

MCMCTree results of divergence times based on ML tree of PCGNT12RNA dataset are shown in Fig. 2 and Table 4 and all detailed results of divergence times estimation are also shown in Figs S11–S16 and Table S5, with a median node height and a 95% highest posterior density (HPD) interval for each node. Here we use the divergence times of Fig. 2 with the range of all divergence times estimated from six trees

for the corresponding nodes to display these results. The early divergence of Reduvioidea from other cimicomorphans could be dated back to 219 Ma (192–225 Ma), and the split between Miroidea and Cimiciformes *sensu lato* was estimated to occur 11 Ma after that event. The Miroidea was estimated to begin to diversify at around 193 Ma (175–200 Ma), with the successive divergence between Miridae and Tingidae taking place at 181 Ma. The early diversification of Miridae occurred at 138 Ma (138–177 Ma), in the Cretaceous, and the hyperdiverse Mirinae radiated after 91 Ma (91–94 Ma), in the Late Cretaceous.

The split between Aradoidea and Trichophora occurred in the Early Jurassic (198 Ma, 198–231 Ma). Pentatomoidea diverged from the remaining trichophorans at 178 Ma (178–225 Ma) and began to diversify around 163 Ma (163–215 Ma). Pyrrhocoroidea diverged from the Eutrichophora at 151 Ma (151–208 Ma). The divergence between Coreoidea and Lygaeoidea was inferred to occur at 144 Ma (144–193 Ma), with subsequent diversification after 112 Ma (112–180 Ma) and 137 Ma (137–176 Ma), respectively. The minimal difference in divergence times of Pyrrhocoroidea and (Coreoidea + Lygaeoidea), and Coreoidea and Lygaeoidea seems to explain the persistent problems with inferring their phylogenetic relationships. Pentatomidae, Coreinae, and Rhyparochromidae each began to diversify in the Late Cretaceous, between 69 and 80 Ma. For convenience we will use the four major phytophagous clades to indicate Mirinae, Pentatomidae, Coreinae, and Rhyparochromidae in the following paragraphs.

Ancestral state reconstruction of feeding habits

The results of ML ancestral character reconstruction of feeding habits based on ML tree of PCGNT12RNA dataset are shown in Fig. 2, and the other results of ML ancestral character reconstruction are also shown in Figs S17–S21. The MRCA of Terheteroptera is hypothesized to exhibit predatory feeding habits. After the divergence of Cimicomorpha and Pentatomomorpha, the feeding strategy has evolved in different ways in each clade. Most cimicomorphan lineages retained the original predatory diet. While the MRCA of Miroidea shifted from predatory to phytophagous habits in all reconstruction results except for those inferred from PCGNT12RNA parsimony-based topology. The ancestral feeding habit of Miridae was likely phytophagous, retained in most of the subfamilies, but predation apparently evolved in the family several times independently (e.g., Isometopinae and Deraeocorinae), as zoophytophagy (e.g., Orthotylinae). Some clades, e.g., Cylapinae, acquired specialized fungivorous feeding habits. As the overwhelming majority of the Pentatomomorpha are phytophagous, this was

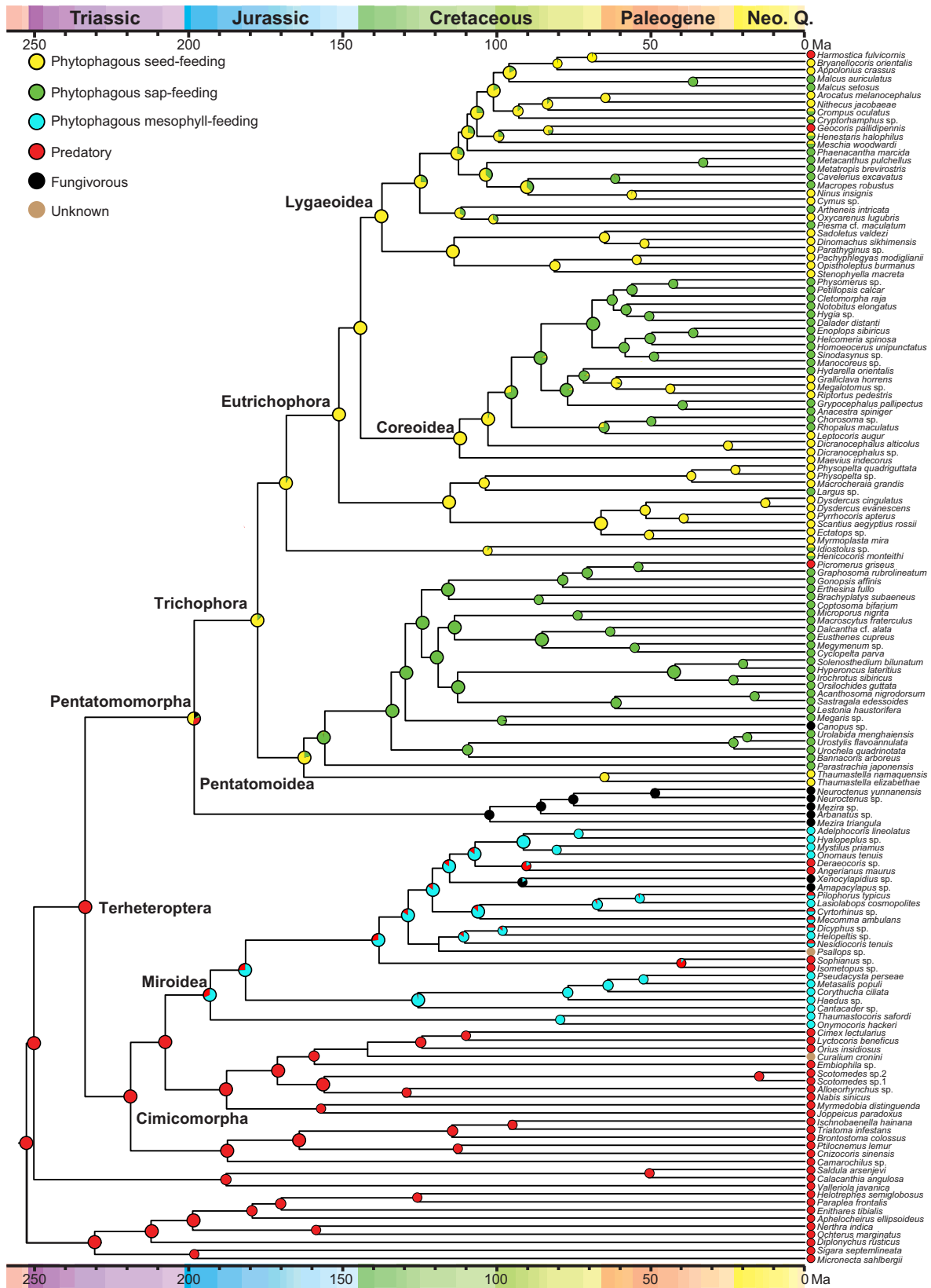


Fig. 2. Estimated divergence times of major terheteropteran lineages based on maximum-likelihood tree inferred from PCGNT12RNA dataset. The pie charts on the nodes and terminals indicate the likelihood ancestral state reconstruction of feeding habit.

likely the ancestral feeding habit for the entire clade or at least of the Trichophora (seed-feeding with 87.1–91.9% proportional likelihood except for result of parsimony-based topology inferred from PCGNT12RNA dataset). Transitions from seed-feeding to sap-feeding occurred in the deep node of Pentatomoidea and that of Coreoidea, respectively, while Lygaeoidea and Pyrrhocoroidea retained the seed-feeding habit in most descendent groups. A few terminal lineages, most notably the Asopinae (within the superfamily Pentatomoidea) and the Geocorinae (within the Lygaeoidea), and Cleradini (within the Lygaeoidea), acquired predatory or hematophagous feeding habits secondarily.

Discussion

Phylogeny of Cimicomorpha and Pentatomomorpha

Based on the newly sequenced data of 100 species, and previously reported data of 50 species together representing a broad sample within Cimicomorpha and Pentatomomorpha, our investigation resulted in a series of well-resolved and supported relationships, corroborating previously recognized backbone of ter-heteropteran phylogeny. The monophyly of both Cimicomorpha and Pentatomomorpha, and their sister relationship suggested by previous authors, based on various morphological and molecular evidence (e.g., Kieran et al., 2019; de Moya et al., 2019; Tian et al., 2008; Wang et al., 2016, 2019; Weirauch et al., 2019; Wheeler et al., 1993), were corroborated with strong support values. The paraphyly of Cimicomorpha

proposed by a few studies based on mitogenomic data (Li et al., 2017; Liu et al., 2018) was not corroborated. Despite using the site-heterogeneous model, the mitochondrial phylogenetics may still suffer from a bias in base composition and mutational rate (Yang et al., 2018). Besides, phylogenetic signals provided by the mitogenome still limit the higher-level reconstruction of insect phylogeny (Song et al., 2016). The established monophyly of Cimicomorpha corroborates the recognition of both micropyles and aeropyles around the operculum of the eggs as a synapomorphy of this infraorder (Weirauch et al., 2019; Wheeler et al., 1993). Prior to this study the phylogenetic relationships within Cimicomorpha had been investigated, with various taxa sampled morphologically and/or molecularly, resulting in different topologies (Schuh & Štys, 1991; Schuh et al., 2009; Tian et al., 2008; Weirauch et al., 2019). Our results support the superfamily-level phylogenetic relationships, namely Reduvoidea + (Miroidea + Cimiciformes *sensu lato*), in concordance with the results reached by previous authors based on morphology (Schuh & Štys, 1991) and combined morphological and molecular data (Weirauch et al., 2019).

Within Miroidea, the relationships of the three families are so far still equivocal. The sister relationship between Miridae and Tingidae was recovered in ML and BI analyses based on the PCGNT12RNA dataset alone. The same topology has also been proposed in previous phylogenetic analyses of morphological or combined data (Schuh & Štys, 1991; Weirauch et al., 2019), which constitute independent support for such a topology. The alternative topologies, ML and BI trees of PCGAARNA dataset (Miridae + Thaumastocoridae) and parsimony trees of PCGNT12RNA and PCGAARNA datasets (Tingidae + Thaumastocoridae), were also recovered by the previous studies (Wang et al., 2016, 2019). The obvious long branch of Thaumastocoridae may lead to the varied topologies in this study. The higher classification of Miridae with eight recognized subfamilies (Cassis & Schuh, 2012) has been generally accepted by the taxonomic community, but with considerable disagreement regarding the phylogenetic relationships among these subfamilies (Jung & Lee, 2012; Lin & Yang, 2005; Schuh, 1976; Schuh et al., 2009; Weirauch et al., 2019). Most morphological analyses (Leston, 1961; Schuh, 1974, 1976) recovered Isometopinae as the sister group of the remainder of the Miridae. Our study reached the same conclusion with the ML, BI and parsimony analyses of the PCGNT12RNA dataset, corroborating the hypothesis that the greatly reduced number of trichobothria on the meso- and metafemora represents an apomorphy for the subfamily, while the presence of ocelli is also a synapomorphy for Isometopinae (Schuh, 1976). Two consistently monophyletic groups within the clade of non-isometopine mirids, already

Table 4
Estimation of divergence times (Ma) based on maximum-likelihood tree inferred from PCGNT12RNA dataset for major groups in this study

Clade	Mean	95% HPD
Cimicomorpha	219	209–228
Reduvoidea	187	166–208
Cimicoidea	159	146–173
Naboidea	156	151–164
Microphysoidea	157	119–185
Miroidea	193	181–204
Miridae	138	127–150
Mirinae	91	88–97
Pentatomomorpha	198	185–211
Pentatomoidea	163	149–176
Pentatomidae	79	63–93
Idiostoloidea	104	71–130
Pyrrhocoroidea	115	99–130
Coreoidea	112	93–131
Coreinae	69	60–78
Lygaeoidea	137	125–149
Rhyparochromidae	80	67–93

proposed by previous authors, were also recovered in the present study; these are Mirinae + Deraeocorinae (Jung & Lee, 2012; Kelton, 1959; Leston, 1961; Schuh, 1974, 1976; Schuh et al., 2009; Slater, 1950) and Orthotylinae + Phylinae (Kelton, 1959; Leston, 1961; Menard et al., 2014; Schuh, 1974, 1976; Schuh et al., 2009; Slater, 1950; Weirauch et al., 2019).

Within the Pentatomomorpha, the sister relationship of Aradoidea and Trichophora was consistent across our analyses and previous studies (Hua et al., 2008; Kieran et al., 2019; Li et al., 2017; Liu et al., 2019; de Moya et al., 2019; Wang et al., 2016; Weirauch et al., 2019). Within the Trichophora our analyses based on PCGNT12RNA dataset suggest a sister relationship between Idiostoloidea and Eutrichophora, supporting the recognition of Idiostoloidea as a separate superfamily (Henry, 1997; Štys, 1964; Weirauch et al., 2019). The relationships of the three Eutrichophora superfamilies have been investigated repeatedly but remain ambiguous. Although the support values of ML and parsimony analyses are low, nearly all our analyses are in favor of Pyrrhocoroidea + (Coreoidea + Lygaeoidea), which was also supported by previous analyses using 18S rDNA (Xie et al., 2005), mitogenome (Hua et al., 2008), ultraconserved element loci (Forthman et al., 2019), and combined rDNA and morphological characters (Weirauch et al., 2019). Besides, investigation of gut symbionts revealed that the *Burkholderia* symbionts of most lygaeoids and coreoids belong to the same lineage, while those of pyrrhocoroids belong to another lineage (Gordon et al., 2016; Kikuchi et al., 2011), also suggesting a close relationship between Coreoidea and Lygaeoidea. These phylogenetic results will have immense impact on our understanding of eutrichophoran morphology. For example, the resultant topology suggests open trichobothrium associated with the trichome (Gao et al., 2017; Hemala et al., 2020; Kment et al., 2019) as a synapomorphy of Eutrichophora, subsequently lost in Coreoidea (except for the Hyocephalidae) and in some Lygaeoidea lineages.

Concerning Pentatomoidea phylogeny, our analyses support Thaumastellidae as representing the earliest split from the ancestral pentatomoid stock, in accordance with the result of 16S rDNA data using the direct optimization method of Grazia et al. (2008) and Weirauch et al. (2019). The clade, including two morphologically very similar families, Saileriolidae and Urostylididae (previously recognized as subfamilies of a more inclusively defined Urostylididae), represents early divergent extant groups, recognized by the analysis of four loci using the direct optimization method of Grazia et al. (2008), Wu et al. (2018) and Weirauch et al. (2019). The phylogenetic positions of Parastrachiidae and Canopidae are still unclear, which might be ascribed to few phylogenetic signals from limited

sequence data. As seen above, Dolling's (1981) hypothesis of Cydnidae *sensu lato* (including Thaumastellidae, Thyreocoridae, Parastrachiidae and Cydnidae *sensu stricto*; see also Schuh & Weirauch, 2020) is rejected, consistently with recent study by Rocacuschs et al. (2022). Lestoniidae + Acanthosomatidae and Cydnidae *sensu stricto* + (Dinidoridae + Tesaratomidae) were also recovered as two well-supported monophyletic groups by our analyses, consistently with previous studies (Grazia et al., 2008; Wu et al., 2018).

Within the Pyrrhocoroidea, our results confirm the monophyly of Largidae, recently doubted by Hemala et al. (2020, 2021) due to lack of morphological evidence, and its sister relationship with Pyrrhocoridae.

Within the Coreoidea, recent phylogenomic results recovered Hydarinae and Pseudophloeinae as clades nested within the Alydidae, resulting in a rejection of the monophylies of both Alydidae and Coreidae (Forthman et al., 2019). This hypothesis is further supported by a recent morphological study of coreoid spermatheca (Pluot-Sigwalt & Moulet, 2020) and the metathoracic scent gland peritreme (Hemala et al., 2021). Therefore, the higher classification of Coreoidea should be revised, with two equally sound alternative solutions: (i) incorporating Alydidae into a broadly defined Coreidae; or (ii) transferring Hydarinae and Pseudophloeinae into Alydidae *sensu lato*. As a five-family taxonomic arrangement of Coreoidea has been generally accepted for decades, the second solution, being more compliant with the established classification, appears more agreeable. It is, however, stressed that a formal reclassification of Coreoidea must rest on an analysis performed on a much broader sample. We also confirm Hyocephalidae and Stenocephalidae as the early divergent groups of extant Coreoidea (cf. Kment et al., 2019).

For Lygaeoidea, our results highly support the sister relationship between (Pachygronthidae + Heterogastridae) and the remaining lygaeoids, differing from previous results of morphological cladistic analysis recovering (Pachygronthidae + Heterogastridae) + Rhyparochromidae as sister group to other lygaeoids (Henry, 1997). In fact, Rhyparochromidae has never been recovered as an early divergent extant group either in molecular (Liu et al., 2019; de Moya et al., 2019; Tian et al., 2011) or in combined analyses (Weirauch et al., 2019). The branch that subsequently split is another well-supported lineage formed by Artheneidae + (Oxycarenidae + Piesmatidae). Although the placement of Piesmatidae has a tortuous history, recent authors universally recognize it as a member of Lygaeoidea (Henry, 1997; Tian et al., 2011; Xie et al., 2005), and a sister relationship with Oxycarenidae has also been proposed (Xie et al., 2005). The supposedly monophyletic 'malcid-line', proposed to comprise

Berytidae, Colobathristidae, Cryptorhamphidae, Cymidae, Malcidae, and Ninidae (Štys, 1967), and subsequently also Piesmatidae (Schaefer, 1975), was recognized in a cladistic analysis based on morphological data (Henry, 1997), but it was recovered neither in our analyses nor in several recent phylogenetic studies (Hua et al., 2008; Liu et al., 2019; de Moya et al., 2019; Weirauch et al., 2019). Of the putative families within the ‘malcid-line’, Ninidae + Cymidae were invariably grouped with Blissidae with high support values, in a way consistent with a previous study based on 18S rDNA (Xie et al., 2005).

Dating the evolutionary history of phytophagous true bugs

For several nodes, the MCMCtree results show relatively large differences in estimated divergence times (Table S5), which is mainly attributed to the different topologies used for analyses. The dissimilar datasets may also be a potential resource for these differences. Comparing the phylogenetic trees reported in this study and previously proposed phylogenies, the ML tree of PCGNT12RNA dataset show the higher consistency

with current view of terheteropteran phylogeny (Table 5), and thus the corresponding results of divergence time estimation may be more credible. This chronogram generally demonstrates the similar estimated divergence times of nodes between superfamilies and families in Cimicomorpha to some of previous studies (Table 1). Our estimated divergence time of Miridae, however, is 139 Ma later than that of Jung and Lee (2012). In the latter analysis, four fossil mirid species were used to calibrate the nodes of four subfamilies, among which *Miridoidea mesozoicus* and *Scutellifer karatavicus* (Herczek & Popov, 2001) were regarded as the oldest known fossils of Orthotylinae and Mirinae, respectively. Recently the taxonomic placement of both fossils was questioned; *M. mesozoicus* was recognized as the oldest fossil mirid, whilst the position of *S. karatavicus* was treated as uncertain (Schuh & Weirauch, 2020). The geologically estimated time span of *M. mesozoicus* (Late Jurassic) is slightly earlier than the phylogenetically estimated time interval of early divergence of the Miridae in our study (138 Ma).

The divergence of the infraorder Pentatomomorpha was found to have occurred at 198 Ma (the Early Jurassic), a result very close to the estimation of Johnson

Table 5
Phylogenetic relationships of major phytophagous lineages derived from this study and references

Clade	Li et al. (2017)	Johnson et al. (2018)	de Moya et al. (2019)	Wang et al. (2019)	Weirauch et al. (2019)	ML analyses	BI analyses	Parsimony analyses
Cimicomorpha	–	Transcriptome	Transcriptome	Transcriptome	M&rDNA	NT12, AA	NT12, AA	NT12, AA
Miroidea	NA	NA	NA	Transcriptome	M&rDNA	NT12, AA	NT12, AA	NT12, AA
TMS + (MIR + TIN) (Schuh & Štys, 1991)	NA	NA	NA	–	M&rDNA	NT12	NT12	–
ISO + other mirids (Schuh, 1976)	NA	NA	NA	NA	–	NT12	NT12	NT12
Pentatomomorpha	MT	Transcriptome	Transcriptome	Transcriptome	M&rDNA	NT12, AA	NT12, AA	NT12, AA
Aradidae + Trichophora (Wheeler et al., 1993)	MT	Transcriptome	Transcriptome	Transcriptome	M&rDNA	NT12, AA	NT12, AA	NT12, AA
Idiostoloidea + Eutrichophora this study	NA	NA	NA	NA	–	NT12	NT12	NT12, AA
PYR + (COR + LYG) (Xie et al., 2005)	–	–	–	–	M&rDNA	NT12, AA	NT12, AA	NT12
Pentatomoidea	MT	Transcriptome	Transcriptome	NA	M&rDNA	NT12, AA	NT12, AA	NT12, AA
THA + other pentatomoids (Weirauch et al., 2019)	NA	NA	NA	NA	M&rDNA	NT12, AA	NT12, AA	AA
Coreoidea	MT	Transcriptome	Transcriptome	NA	M&rDNA	NT12, AA	NT12, AA	NT12, AA
PSE + Alydinae (Forthman et al., 2019)	NA	NA	NA	NA	NA	NT12, AA	NT12, AA	NT12, AA
Lygaeoidea	MT	Transcriptome	Transcriptome	NA	M&rDNA	NT12, AA	NT12, AA	NT12, AA
(PAC + HET) + other lygaeoids (Tian et al., 2011)	NA	NA	NA	NA	NA	NT12, AA	NT12, AA	NT12, AA

AA, PCGAARNA dataset; ALY: Alydinae; COR: Coreoidea; Dashes, not recovered; HET: Heterogastridae; ISO: Isometopinae; LYG: Lygaeoidea; M&rDNA, combined morphological and rDNA data; MIR: Miridae; MT: mitogenome data; NA, not tested; NT12, PCGNT12RNA dataset; PAC: Pachygronthidae; PSE: Pseudophloeinae; PYR: Pyrrhocoroidea; THA: Thaumastellidae; TIN: Tingidae; TMS: Thaumastocoridae.

et al. (2018) (200 Ma). The estimated times from most other previous studies varied from 153 Ma to 237 Ma (Table 1), while fossils of Pentatomomorpha are known from as early as the Late Triassic: *Pachymerus zucholdi* (Pachymeridiidae) from the Rhaetian Stage, 201.3–208.5 Ma (Giebel, 1856; Schuh & Weirauch, 2020), apparently supporting the results around the boundary of the Triassic and Jurassic. Our analyses showed Pentatomoidea diverged in the Jurassic, and that of the superfamilies Coreoidea, Lygaeoidea, Pyrrhocoroidea and Idiostoloidea appeared in the Early Cretaceous. The mean estimated ages of extant groups of these superfamilies recovered by previous studies largely conflicted with each other, ranging from the Late Jurassic to Early Cretaceous for each superfamily node (Table 1), and the divergence times between families of Pentatomomorpha were also inconsistent. In fact, the earliest fossil which can be unambiguously placed in the Pentatomoidea is *Mesopentacoris orientalis* (Mesopentacoridae) from the Middle Jurassic, 166–170 Ma (Popov, 1989; Schuh & Weirauch, 2020). Additionally, credible fossils of Coreoidea and Idiostoloidea can be dated back to the Early Cretaceous (Schuh & Weirauch, 2020), indicating that our estimated ages are in better agreement with the fossil record for the majority of the Pentatomomorpha nodes.

Comparing the results of ancestral state reconstruction of feeding habits with previous studies, both ten (Weirauch et al., 2019) and five feeding types for ancestral state reconstruction of feeding habits show similar results of the origin of phytophagy and most deep nodes within Pentatomomorpha and Cimicomorpha. The different feeding types used in ancestral state reconstruction may make direct impact more regularly on shallow nodes. Combining divergence time estimation with an ancestral state reconstruction of feeding habits, three phases in the evolutionary history of phytophagous true bugs can be recognized. Although divergence times inferred from ML tree of PCGNT12RNA dataset with more confidence mentioned above, we still integrated all six MCMCTree results of divergence time estimation to display a more credible and stable evolutionary pattern of phytophagous true bugs. Along with the independent origin of phytophagy within the Cimicomorpha and Pentatomomorpha, the potentially earliest boundary of the shift to phytophagy in Pentatomomorpha is 198 Ma (198–231 Ma), and Cimicomorpha is 193 Ma (175–200 Ma). In Pentatomomorpha, phytophagy was acquired no later than 178 Ma (178–225 Ma; the MRCA of Trichophora). After the initial emergences of the above lineages, phytophagous true bugs diversified smoothly during the Jurassic, with the emergence of the most trichophoran superfamilies and three miroid families. During the Early Cretaceous, phytophagous true bugs underwent a rapid radiation phase (Fig. 3), resulting in the establishment of most extant and extinct

families of the Trichophora and most of the present subfamilies of the Miroidea. Within the third phase (after the Early Cretaceous), the family- and subfamily-level diversification rate of phytophagous true bugs gradually decreased. The diversification of the four major phytophagous clades (Mirinae, Pentatomidae, Coreinae, and Rhyparochromidae) within the major phytophagous superfamilies (Miroidea, Pentatomoidea, Coreoidea, and Lygaeoidea) mainly occurred in the Late Cretaceous.

Patterns and driving forces of the diversification of phytophagous true bugs

Phytophagous lineages account for more than 60% of the total species level diversity of Heteroptera. Its members occupy all terrestrial habitats where plants are present. Phytophagy is therefore apparently a vital factor in the diversification of true bugs. The evolutionary process and essential drivers of the diversification of phytophagous true bugs have remained poorly understood in comparison with those of various predatory groups of the order, such as the true water bugs (Wang et al., 2021; Ye et al., 2020) or assassin bugs (Hwang & Weirauch, 2012; Zhang et al., 2016). In the present study we combined our results of the inferred evolutionary history of the group with information currently available on paleoenvironmental and paleoclimatic history, as well as angiosperm evolution, to investigate the patterns and driving forces of diversification in phytophagous true bugs.

Among the five well-known mass extinctions that took place during the Phanerozoic, the Permian-Triassic boundary event (PTB) was the most destructive, resulting in a substantial reduction in marine (Raup, 1979), terrestrial vertebrate (Maxwell, 1992) and insect fauna (Labandeira & Sepkoski, 1993) as well as in plants (McElwain & Punyasena, 2007). A gradual recovery of terrestrial fauna from the PTB mass extinction occurred during the Early and Middle Triassic (Grauvogel-Stamm & Ash, 2005; Irmis & Whiteside, 2012; Shcherbakov, 2008). The earliest reliable angiosperm fossil can be dated back to the Early Cretaceous, i.e., the microfossils pollen grains found in the Valanginian-Hauterivian Stage (129–139 Ma; Brenner, 1996; Hughes & McDougall, 1987; Hughes et al., 1991) and the macrofossils reported from the Barremian–earliest Aptin (124–129 Ma; Friis et al., 2006; Li, 2003; Sun et al., 1998). There is no reliable pre-Cretaceous angiosperm fossil described to date, while recent phylogenomic studies have consistently confirmed that the early divergence of angiosperms occurred in the Triassic (207–248 Ma; Barba-Montoya et al., 2018; Li et al., 2019a; Yang et al., 2020; Zhang et al., 2020), which implies the really older angiosperm fossils in pre-Cretaceous may not have been recovered or identified yet. Phytophagous

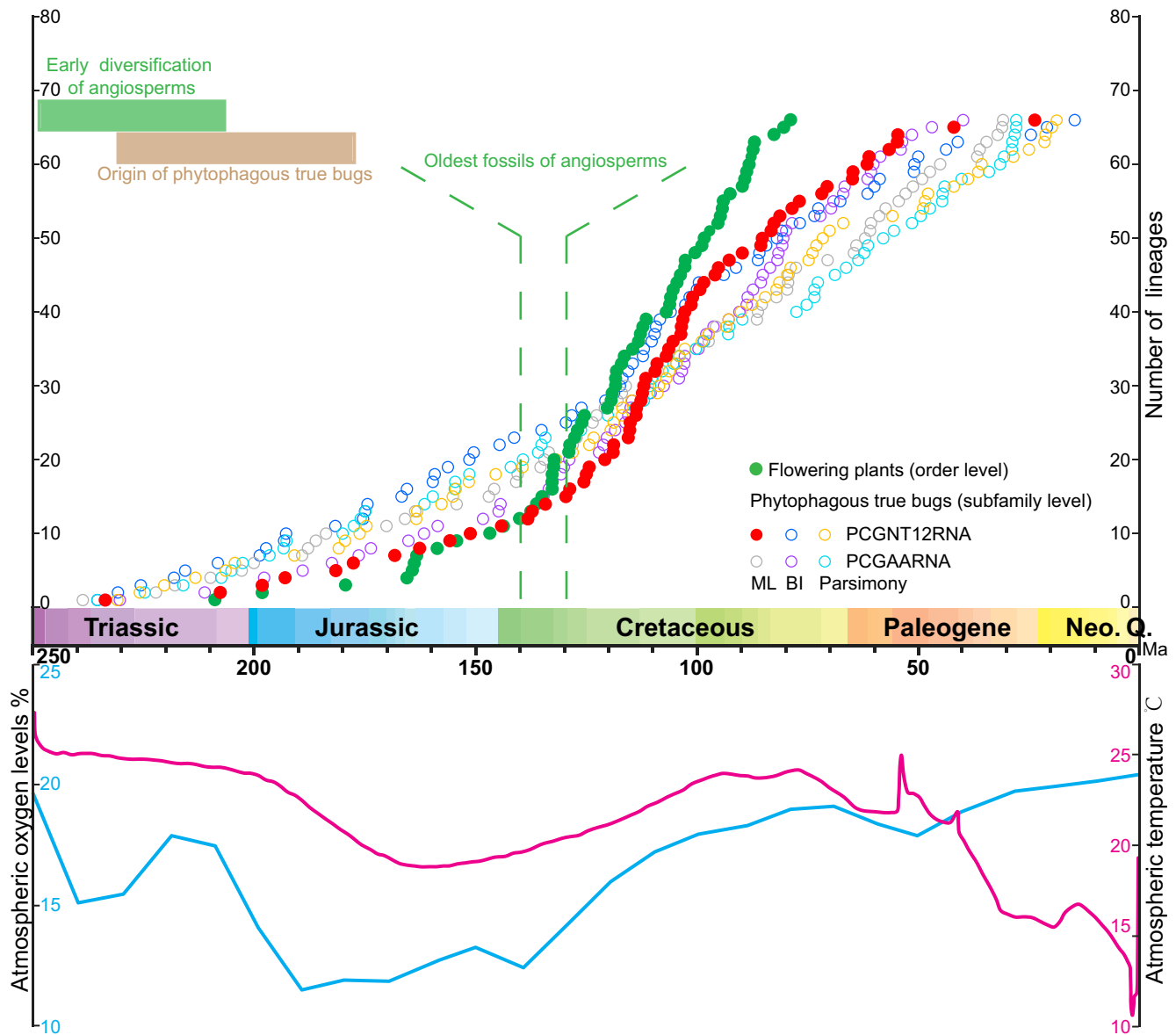


Fig. 3. The lineage-through-time (LTT) plots of phytophagous true bugs and flowering plants based pruned subfamily-level chronogram and order-level chronogram (Li et al., 2019a). The history of global temperature (<http://www.scotese.com/climate.htm>) and atmospheric oxygen level (Ward, 2006) are shown below the LTT plots.

true bugs may arise in the Late Triassic to the Early Jurassic (Fig. 3), being relatively posterior to the early divergence of angiosperms (the Triassic).

Apart from the PTB event, two additional mass extinction events took place in or around the Mesozoic: one in the Triassic-Jurassic boundary (TJB) and another in the Cretaceous-Paleogene boundary. During the extinction event happened in the Jurassic-Cretaceous boundary (Tennant et al., 2016), neither the plants nor the insects were seriously affected (Cascales-Miñana & Cleal, 2014; Dmitriev et al., 2018; Grimaldi & Engel, 2005). The plant LTT plot based

on the reported chronogram (Li et al., 2019a) reveals that angiosperms underwent an explosive radiation during the Early Cretaceous, and the true bugs LTT plots based on all inferred chronograms consistently show the phytophagous true bugs also experienced a rapid diversification phase shortly after that of angiosperms (Fig. 3). The angiosperms completed their order-level diversification in the Late Cretaceous, while the phytophagous true bugs exhibited a slightly lower diversification rate at family and subfamily level in the same period, which result might be associated with the less comprehensive taxon sampling at subfamily level.

The diversification of the four major phytophagous clades proceeded simultaneously during the Late Cretaceous.

Plant-feeding insects frequently undergo reproductive isolation after colonizing a novel host plant, resulting in speciation (Favret & Voegtlin, 2004); therefore, phytophagous insects are generally younger than their host plant lineages (Percy et al., 2004; Tilmon, 2008). Many phytophagous insects follow this evolutionary pattern, especially for higher categories. Only strict insect-plant coevolution groups, e.g., fig-pollinating wasps (Cruaud et al., 2012), show strong contemporaneous diversification patterns. Asynchronous radiations of the phytophagous true bugs and the angiosperms with similar diversification rates during the Early Cretaceous indicate that the angiosperm explosion was an important biotic driving force for the evolution of phytophagous true bugs. Members of most of the extant phytophagous lineages feed on host plants belonging to several taxonomically unrelated plant clades, but a few lineages are indeed closely associated with specific plant lineages, such as all members of Xylastodorinae (Miroidea: Thaumastocoridae), which develop only on palms (Couturier et al., 1998; van Doesburg et al., 2010; Schuh & Weirauch, 2020), or the majority of blissids (Lygaeoidea: Blissidae), which are associated with Poaceae (Schuh & Weirauch, 2020; Slater, 1976). These lineages exhibit strong affinity with host-plant lineages (Couturier et al., 1998; Slater, 1976), and the correlated diversification patterns of the angiosperm lineages and the associated true bug clades can be explored.

Spatio-temporal variations in abiotic factors of the environment and climate have long been considered to play significant roles in biological evolution through geological time (Condamine et al., 2013; Lewitus & Morlon, 2018). The global atmospheric oxygen level rose and hit the Triassic peak during the inferred early diversification phase of the angiosperms and early origin phase of phytophagous true bugs, under a warm climate (Ward, 2006; <http://www.scotese.com/climate.htm>; Fig. 3). From the end-Triassic (Rhaetian) to the Early Jurassic the global atmospheric oxygen level and temperature dropped precipitously; simultaneously the Earth suffered the fourth biodiversity crisis, the TJB mass extinction. From the Late Jurassic global temperature began to rise steadily, with an increase in the atmospheric oxygen level. From the Jurassic to the Cretaceous was the only period of the Mesozoic without mass extinctions, and the continuous steady and recovering environment offered optimal conditions for flourishing plant and insect life. The rapid explosion of phytophagous true bugs in the Early Cretaceous suggests that, along with rising temperature, an increasing atmospheric oxygen level could facilitate—rather than inhibit—biodiversification (Edwards et al., 2017;

Reinhard et al., 2016; Wang et al., 2019). The explosive radiation of angiosperms in the Cretaceous occurred with the continuously rising temperature, indicating a close correlation between biodiversity and global temperature (Mayhew et al., 2008). The remarkable congruence between the rising atmospheric oxygen level and temperature and the rapid diversification of phytophagous true bugs suggests that paleoenvironmental and paleoclimatic changes, especially atmospheric oxygen level, might have promoted the evolution for phytophagous true bugs.

Divergence time estimation and ancestral state reconstruction of feeding habits implies a potentially parallel origin and Early-Cretaceous fast radiation of phytophagous lineages between Miroidea and Pentatomomorpha, and indeed the separate evolutionary histories of these two major lineages have apparently resulted in distinct traits of phytophagy in these groups. The great majority of phytophagous miroid species feed mainly on actively growing tissues of vegetative and generative parts, in particular the mesophyll tissues in the leaves (Wheeler, 2001), while most lygaeoids, pyrrhocorids, and members of the early divergent lineages of Pentatomoidea and Coreoidea generally feed on nearly mature and/or dry seeds. Apart from seed feeders, most of the remaining phytophagous Trichophora feed in the plant circulatory system including underground plant organs, primarily roots. All these significant differences of feeding habits between phytophagous miroids and pentatomomorphans are also reflected by the feeding mechanisms and structure and composition of digestive system. Miroidea bugs are cell-rupture feeders, while most sap-feeding pentatomomorphans are salivary sheath feeders or osmotic pump feeders (Panizzi et al., 2021). Meanwhile, most miroids do not produce the gelling saliva that is present in the salivary range of pentatomomorphans (Panizzi et al., 2021; Sharma et al., 2014). In addition, the salivary gland organs of miroids possess the accessory salivary gland vesicles serving the recirculation of water to keep a flow of saliva, which is absent in pentatomomorphans. In fact, cell-rupture feeders generally do not suffer from a great excess of water during feeding process, while the gastric caeca system as a water eliminating system allows sap-sucking pentatomomorphans to metabolize the excess water, a feature which is absent in miroids (Goodchild, 1963). Besides, there also exist differences in the mouthpart structures of true bugs with various feeding preference (Cobben, 1978; Wang et al., 2020).

The distribution and frequency of transformation of feeding habits within Miroidea and Trichophora are quite different. Of Miroidea, the Tingidae and Thaumastocoridae are exclusively phytophagous lineages. Within the Miridae, which accounts for over 80% of the diversity of Miroidea (Henry, 2017), one can

observe the evolution from phytophagy to zoophagy across nearly all the subfamilies: the apparent sister group of the remaining Miridae, Isometopinae, is zoophagous, and many genera or species from several other subfamilies such as Orthotylinae and Deraeocorinae are zoophagous or zoophytophagous. Yet, the Bryocorinae, Mirinae and Phylinae are predominantly or exclusively phytophagous with a few glaring exceptions e.g., the zoophytophagous Dicyphini of Bryocorinae and the genus *Phytocoris* of Mirinae (Schuh & Weirauch, 2020; Wheeler, 2001). In contrast, Trichophora retained phytophagy as the primary diet for the nearly all lineages during their evolution. The three major pentatomomorphan superfamilies almost universally retained phytophagy, except for three well-defined lineages which secondarily shifted to zoophagy: Asopinae (Pentatomoidea), Geocorinae, and Cleradini (both Lygaeoidea), the last of which even became hematophagous (Schuh & Weirauch, 2020), and a few predaceous Pyrrhocoridae (Ahmad & Schaefer, 1987) and zoophytophagous Berytidae species (Morkel, 2007). Despite the evolution of phytophagy acquisition, the mechanism of feeding behavior and the establishment of a preferred plant part, exhibiting distinct pattern differences between the Miroidea and Pentatomomorpha, similar diversification trends dominate the independent evolutionary processes and pattern for phytophagous true bugs within two infraorders.

In conclusion, we reconstructed the phylogenetic relationships within Terheteroptera (Cimicomorpha + Pentatomomorpha) based on 138 ingroups representing 90% of terheteropteran family-level diversity using ML, BI, and parsimony methods; in so doing we recovered a robust scheme of superfamily-level relationships, i.e., (Reduivoidea + (Miroidea + (Microphysoidea + (Cimicoidea + Naboidae)))) + (Aradoidea + (Pentatomoidea + (Idiostoloidea + (Pyrrhocoroidea + (Coreoidea + Lygaeoidea))))). This study provides an evolutionary timescale for Terheteroptera and an ancestral state reconstruction of their feeding habits and supports that phytophagous true bugs underwent a family-level rapid adaptative radiation in the Early Cretaceous. The best possible evidence to date, i.e., the inferred scenario of phytophagous true bugs evolving together with the angiosperms, along with the paleoenvironmental and paleoclimatic history, supports the hypothesis that angiosperm radiation and increasing atmospheric oxygen level could be important biotic and abiotic drivers for the diversification of phytophagous true bugs, respectively.

Acknowledgements

This project was supported by the National Natural Science Foundation of China (grant numbers: 31222051,

31572242, 31772425). The work of PK was supported by the Ministry of Culture of the Czech Republic (DKRVO 2019–2023/5.I.d, National Museum, 00023272).

Conflict of interest

The authors declare that they have no conflicting interests.

Data Availability Statement

The authors confirm that the data supporting the findings of this study are available within the article and its supplementary materials.

References

- Abascal, F., Zardoya, R. & Telford, M.J. (2010) TranslatorX: multiple alignment of nucleotide sequences guided by amino acid translations. *Nucleic Acids Research*, 38, W7–W13.
- Ahmad, I. & Schaefer, C.W. (1987) Food plants and feeding biology of the Pyrrhocoroidea (Hemiptera). *Phytophaga*, 1, 75–92.
- Allen, J.M., LaFrance, R., Folk, R.A., Johnson, K.P. & Guralnick, R.P. (2018) aTRAM 2.0: an improved, flexible locus assembler for NGS data. *Evolutionary Bioinformatics*, 14, 1–4.
- Bae, S.D., Kim, H.J. & Mainali, B.P. (2014) Infestation of *Riptortus pedestris* (Fabricius) decreases the nutritional quality and germination potential of soybean seeds. *Journal of Asia-Pacific Entomology*, 17, 477–481.
- Barba-Montoya, J., Dos Reis, M., Schneider, H., Donoghue, P.C.J. & Yang, Z. (2018) Constraining uncertainty in the timescale of angiosperm evolution and the veracity of a Cretaceous Terrestrial Revolution. *New Phytologist*, 218, 819–834.
- Becker-Migdisova, E.E. (1962). Order Heteroptera: Heteropterans, or True Bugs, in *Osnovy paleontologii*. Tom 9. In: Rohdendorf, B.B. (Ed.), *Chlenistonogie. Trakheinye i kheliterovye* (Fundamentals of Paleontology: Vol. 9. Arthropoda: Tracheata and Chelicerata), Moscow: Akad. Nauk SSSR, pp. 217–224.
- Brenner, G. (1996) Evidence for the earliest stage of angiosperm pollen evolution: a paleo-equatorial section from Israel. In: Taylor, D. & Hickey, L. (Eds.) *Flowering plant origin, evolution and phylogeny*. New York: Chapman & Hall, pp. 91–115.
- Camacho, C., Coulouris, G., Avagyan, V., Ma, N., Papadopoulos, J., Bealer, K. et al (2009) BLAST+: architecture and applications. *BMC Bioinformatics*, 10, 421.
- Cascales-Miñana, B. & Cleal, C. (2014) The plant fossil record reflects just two great extinction events. *Terra Nova*, 26, 195–200.
- Cassis, G. & Schuh, R.T. (2012) Systematics, biodiversity, biogeography, and host associations of the Miridae (Insecta: Hemiptera: Heteroptera: Cimicomorpha). *Annual Review of Entomology*, 57, 377–404.
- Cobben, R.H. (1978) Evolutionary trends in Heteroptera. Part II. Mouthpart structures and feeding strategies. *Agricultural Research Reports*, 78–5, 1–407.
- Cockerell, T.D.A. (1921) Some Eocene insects from Colorado and Wyoming. *Proceedings of the United States National Museum*, 59, 29–39.
- Condamine, F.L., Rolland, J. & Morlon, H. (2013) Macroevolutionary perspectives to environmental change. *Ecology Letters*, 16, 72–85.
- Couturier, G., Kahn, F. & Padilha de Oliveira, M.D.S. (1998) New evidences on the coevolution between bugs (Hemiptera: Thaumastocoridae: Xylastodorinae) and the New World palms. *Annales de la Société Entomologique de France*, 34(1), 99–101.
- Cruaud, A., Rønsted, N., Chantarasuwan, B., Chou, L.S., Clement, W.L., Couloux, A. et al (2012) An extreme case of plant-insect

- codiversification: figs and fig-pollinating wasps. *Systematic Biology*, 61, 1029–1047.
- Dmitriev, V.Y., Aristov, D.S., Bashkuev, A.S., Vasilenko, D.V., Vřánský, P., Gorochovc, A.V. et al (2018) Insect diversity from the Carboniferous to Recent. *Paleontological Journal*, 52, 610–619.
- Dolling, W.R. (1981) A rationalized classification of the burrower bugs (Cydniidae). *Systematic Entomology*, 6, 61–76.
- Edwards, C.T., Saltzman, M.R., Royer, D.L. & Fike, D.A. (2017) Oxygenation as a driver of the great Ordovician biodiversification event. *Nature Geoscience*, 10, 925–929.
- Favret, C. & Voegtlin, D.J. (2004) Speciation by host-switching in pinyon *Cinara* (Insecta: Hemiptera: Aphididae). *Molecular Phylogenetics and Evolution*, 32(1), 139–151.
- Forthman, M., Miller, C.W. & Kimball, R.T. (2019) Phylogenomic analysis suggests Coreidae and Alydidae (Hemiptera: Heteroptera) are not monophyletic. *Zoologica Scripta*, 48, 520–534.
- Friis, E.M., Pedersen, K.R. & Crane, P.R. (2006) Cretaceous angiosperm flowers: innovation and evolution in plant reproduction. *Palaeogeography, Palaeoclimatology, Palaeoecology*, 232(2–4), 251–293.
- Fujiyama, I. (1987) Middle Miocene insect fauna of Abura, Hokkaido, Japan, with notes on the occurrence of Cenozoic fossil insects in the Oshima Peninsula, Hokkaido. *Memoirs of the National Science Museum*, 20, 37–43.
- Gao, C., Rédei, D., Shi, X., Cai, B., Liang, K., Gao, S. et al (2017) A comparative study of the abdominal trichobothria of Trichophora, with emphasis on Lygaeoidea (Hemiptera: Heteroptera). *European Journal of Entomology*, 114, 587–602.
- Giebel, C.G. (1856). *Fauna der Vorwelt mit steter Berücksichtigung der lebenden Thiere. Zweiter Band: Gliederthiere. Erste Abtheilung: Insecten und Spinnen.* Leipzig: Brockhaus.
- Goloboff, P.A. & Catalano, S.A. (2016) TNT version 1.5, including a full implementation of phylogenetic morphometrics. *Cladistics*, 32, 221–238.
- Goodchild, A.J.P. (1963) Studies on the functional anatomy of the intestines of Heteroptera. *Proceedings of the Zoological Society of London*, 141, 851–910.
- Gordon, E.R., McFrederick, Q. & Weirauch, C. (2016) Phylogenetic evidence for ancient and persistent environmental symbiont reacquisition in Largidae (Hemiptera: Heteroptera). *Applied and Environment Microbiology*, 82, 7123–7133.
- Grabherr, M.G., Haas, B.J., Yassour, M., Levin, J.Z., Thompson, D.A., Amit, I. et al (2011) Full-length transcriptome assembly from RNA-Seq data without a reference genome. *Nature Biotechnology*, 29, 644–652.
- Grauvogel-Stamm, L. & Ash, S.R. (2005) Recovery of the Triassic land flora from the end-Permian life crisis. *Comptes Rendus Palevol*, 4, 593–608.
- Grazia, J., Schuh, R.T. & Wheeler, W.C. (2008) Phylogenetic relationships of family groups in Pentatomoidea based on morphology and DNA sequences (Insecta: Heteroptera). *Cladistics*, 24, 932–976.
- Grimaldi, D. & Engel, M.S. (2005) *Evolution of insects.* Cambridge, UK: Cambridge University Press.
- Hamilton, G.C., Ahn, J.J., Bu, W.-J., Leskey, T.C., Nielsen, A.L., Park, Y.-L. et al (2018). *Halyomorpha halys* (Stal). In: McPherson, J.E. (Ed.). *Invasive stink bugs and related species (Pentatomoidea): Biology, higher systematics, semiochemistry, and management.* Boca Raton, London, New York: CRC Press, Taylor & Francis Group, pp. 243–292.
- Heiss, E. & Poinar, G.O. (2012) New Aradidae in Mesozoic Burmese amber (Hemiptera, Heteroptera). *Annalen des Naturhistorischen Museums in Wien, Serie A*, 114, 307–316.
- Hemala, V., Kment, P. & Malenovský, I. (2020) The comparative morphology of adult pregenital abdominal ventrites and trichobothria in Pyrrhocoroidea (Hemiptera: Heteroptera: Pentatomomorpha). *Zoologischer Anzeiger*, 284, 88–117.
- Hemala, V., Kment, P., Tihlaříková, E., Neděla, V. & Malenovský, I. (2021) External structures of the metathoracic scent gland efferent system in the true bug superfamily Pyrrhocoroidea (Hemiptera: Heteroptera: Pentatomomorpha). *Arthropod Structure & Development*, 63(101058), 1–25.
- Henry, T.J. (1997) Phylogenetic analysis of family groups within the infraorder Pentatomomorpha (Hemiptera: Heteroptera), with emphasis on the Lygaeoidea. *Annals of the Entomological Society of America*, 90, 275–301.
- Henry, T.J. (2017) Biodiversity of Heteroptera. In: Footitt, R.G. & Adler, P.H. (Eds.) *Insect biodiversity: science and society*, 2nd edition. Oxford: Wiley-Blackwell, pp. 279–335.
- Herczek, A. & Popov, Y. (2001) Redescription of the oldest plant bugs from the Upper Jurassic of the southern Kazakhstan (Heteroptera: Cimicomorpha, Miridae). *Annals of the Upper Silesian Museum in Bytom, Entomology*, 10–11, 121–128.
- Hoang, D.T., Chernomor, O., Von Haeseler, A., Minh, B.Q. & Vinh, L.S. (2018) UFBoot2: improving the ultrafast bootstrap approximation. *Molecular Biology and Evolution*, 35, 518–522.
- Hua, J., Li, M., Dong, P., Cui, Y., Xie, Q. & Bu, W. (2008) Comparative and phylogenomic studies on the mitochondrial genomes of Pentatomomorpha (Insecta: Hemiptera: Heteroptera). *BMC Genomics*, 9, 610.
- Hughes, N.F. & McDougall, A.B. (1987) Records of angiosperm pollen entry into the English Early Cretaceous succession. *Review of Palaeobotany and Palynology*, 50, 255–272.
- Hughes, N.F., McDougall, A.B. & Chapman, J. (1991) Exceptional new record of Cretaceous Hauterivian angiosperm pollen from southern England. *Journal of Micropalaeontology*, 10, 75–82.
- Hwang, W.S. & Weirauch, C. (2012) Evolutionary history of assassin bugs (Insecta: Hemiptera: Reduviidae): insights from divergence dating and ancestral state reconstruction. *PLoS One*, 7, e45523.
- Irmis, R.B. & Whiteside, J.H. (2012) Delayed recovery of non-marine tetrapods after the end-Permian mass extinction tracks global carbon cycle. *Proceedings of the Royal Society B: Biological Sciences*, 279, 1310–1318.
- Janz, N. & Nylin, S. (1998) Butterflies and plants: a phylogenetic study. *Evolution*, 52, 486–502.
- Janz, N., Nylin, S. & Wahlberg, N. (2006) Diversity begets diversity: host expansions and the diversification of plant-feeding insects. *BMC Evolutionary Biology*, 6, 4.
- Johnson, K.P., Dietrich, C.H., Friedrich, F., Beutel, R.G., Wipfler, B., Peters, R.S. et al (2018) Phylogenomics and the evolution of hemipteroid insects. *Proceedings of the National Academy of Sciences of the United States of America*, 115, 12775–12780.
- Jung, S. & Lee, S. (2012) Molecular phylogeny of the plant bugs (Heteroptera: Miridae) and the evolution of feeding habits. *Cladistics*, 28, 50–79.
- Kalyaanamoorthy, S., Minh, B.Q., Wong, T.K., Von Haeseler, A. & Jermini, L.S. (2017) ModelFinder: fast model selection for accurate phylogenetic estimates. *Nature Methods*, 14, 587–589.
- Katoh, K. & Standley, D.M. (2013) MAFFT multiple sequence alignment software version 7: improvements in performance and usability. *Molecular Biology and Evolution*, 30, 772–780.
- Kelton, L.A. (1959) Male genitalia as taxonomic characters in the Miridae (Hemiptera). *The Canadian Entomologist*, 11, 1–72.
- Kieran, T.J., Gordon, E.R.L., Forthman, M., Hoey-Chamberlain, R., Kimball, R.T., Faircloth, B.C. et al (2019) Insight from an ultraconserved element bait set designed for hemipteran phylogenetics integrated with genomic resources. *Molecular Phylogenetics and Evolution*, 130, 297–303.
- Kikuchi, Y., Hosokawa, T. & Fukatsu, T. (2011) An ancient but promiscuous host-symbiont association between *Burkholderia* gut symbionts and their heteropteran hosts. *ISME Journal*, 5, 446–460.
- Kim, J., Lim, H.-S. & Jung, S. (2021) A first member of bamboo-feeding lineage plant bug (Hemiptera: Heteroptera: Miridae: Mecistoscellini) in mid-Cretaceous Burmese amber. *Cretaceous Research*, 121, 104741.
- Kment, P., Hemala, V. & Malenovský, I. (2019) Scanning the Hyccephalidae: details of their external morphology with respect to phylogenetic relationships within Eutrichophora (Hemiptera: Heteroptera). *Acta Entomologica Musei Nationalis Pragae*, 59, 423–441.

- Labandeira, C.C. & Sepkoski, J.J. Jr (1993) Insect diversity in the fossil record. *Science*, 261, 310–315.
- Layton, M.B. (2000) Biology and damage of the tarnished plant bug, *Lygus lineolaris*, in cotton. *Southwest. Entomology Supplies*, 23, 7–20.
- Leskey, T.C., Hamilton, G.C., Nielsen, A.L., Polk, D.F., Rodriguez-Saona, C., Bergh, J.C. et al (2012) Pest status of the brown marmorated stink bug, *Halyomorpha halys* in the USA. *Outlooks on Pest Management*, 23, 218–226.
- Leston, D. (1961) Testis follicle number and the higher systematics of Miridae (Hemiptera-Heteroptera). *Proceedings Zoological Society of London*, 137, 89–106.
- Lewitus, E. & Morlon, H. (2018) Detecting environment-dependent diversification from phylogenies: a simulation study and some empirical illustrations. *Systematic Biology*, 67, 576–593.
- Li, H. (2003) Lower Cretaceous angiosperm leaf from Wuhe in Anhui, China. *Chinese Science Bulletin*, 48, 611–614.
- Li, H., Leavengood, J.M., Chapman, E.G., Burkhardt, D., Song, F., Jiang, P. et al (2017) Mitochondrial phylogenomics of Hemiptera reveals adaptive innovations driving the diversification of true bugs. *Proceedings of the Royal Society B: Biological Sciences*, 284, 20171223.
- Li, H.T., Yi, T.S., Gao, L.M., Ma, P.F., Zhang, T., Yang, J.B. et al (2019a) Origin of angiosperms and the puzzle of the Jurassic gap. *Nature Plants*, 5, 461–470.
- Li, K., Zhang, X., Guo, J., Penn, H., Wu, T., Li, L. et al (2019b) Feeding of *Riptortus pedestris* on soybean plants, the primary cause of soybean staygreen syndrome in the Huang-Huai-Hai river basin. *The Crop Journal*, 7, 360–367.
- Li, M., Tian, Y., Zhao, Y. & Bu, W. (2012) Higher level phylogeny and the first divergence time estimation of Heteroptera (Insecta: Hemiptera) based on multiple genes. *PLoS One*, 7, e32152.
- Li, M., Wang, Y., Xie, Q., Tian, X., Li, T., Zhang, H. et al (2016) Reanalysis of the phylogenetic relationships of the Pentatomomorpha (Hemiptera: Heteroptera) based on ribosomal, Hox and mitochondrial genes. *Entomotaxonomia*, 38, 81–91.
- Li, T., Gao, C., Cui, Y., Xie, Q. & Bu, W. (2013) The complete mitochondrial genome of the stalk-eyed bug *Chauliops fallax* Scott, and the monophyly of Malcidae (Hemiptera: Heteroptera). *PLoS One*, 8, e55381.
- Lin, C.S. & Yang, C.T. (2005) External male genitalia of the Miridae (Hemiptera: Heteroptera). *National Museum of Natural History Taiwan Special Publication*, 9, 1–174.
- Lin, Q.B. (1977) Fossil insects from Yunnan. *Mesozoic Fossils from Yunnan*, 2, 373–382.
- Lis, J.A., Ziaja, D.J., Lis, B. & Gradowska, P. (2017) Non-monophyly of the “cydnoid” complex within Pentatomoidea (Hemiptera: Heteroptera) revealed by Bayesian phylogenetic analysis of nuclear rDNA sequences. *Arthropod Systematics & Phylogeny*, 75, 481–496.
- Liu, Y., Li, H., Song, F., Zhao, Y., Wilson, J.J. & Cai, W. (2019) Higher-level phylogeny and evolutionary history of Pentatomomorpha (Hemiptera: Heteroptera) inferred from mitochondrial genome sequences. *Systematic Entomology*, 44, 810–819.
- Liu, Y., Song, F., Jiang, P., Wilson, J.J., Cai, W. & Li, H. (2018) Compositional heterogeneity in true bug mitochondrial phylogenomics. *Molecular Phylogenetics and Evolution*, 118, 135–144.
- Lu, Y., Wu, K., Jiang, Y., Xia, B., Li, P., Feng, H. et al (2010) Mirid bug outbreaks in multiple crops correlated with wide-scale adoption of Bt cotton in China. *Science*, 328, 1151–1154.
- Maddison, W.P. & Maddison, D.R. (2019). *Mesquite: a modular system for evolutionary analysis*. Version 3.61, Available at: <http://mesquiteproject.org>
- Maxwell, W.D. (1992) Permian and early Triassic extinction of non-marine tetrapods. *Palaentology*, 35, 571–583.
- Mayhew, P.J., Jenkins, G.B. & Benton, T.G. (2008) A long-term association between global temperature and biodiversity, origination and extinction in the fossil record. *Proceedings of the Royal Society B: Biological Sciences*, 275, 47–53.
- McElwain, J.C. & Punyasena, S.W. (2007) Mass extinction events and the plant fossil record. *Trends in Ecology & Evolution*, 22, 548–557.
- Menard, K.L., Schuh, R.T. & Woolley, J.B. (2014) Total-evidence phylogenetic analysis and reclassification of the Phylinae (Insecta: Heteroptera: Miridae), with the recognition of new tribes and subtribes and a redefinition of Phylini. *Cladistics*, 30, 391–427.
- Morkel, C. (2007) On kleptoparasitic stilt bugs (Insecta, Heteroptera: Berytidae) in spider funnel-webs (Arachnida, Araneae: Agelenidae), with notes on their origin. *Mainzer Naturwissenschaftliches Archiv, Beiheft*, 31, 129–143.
- de Moya, R.S., Weirauch, C., Sweet, A.D., Skinner, R.K., Walden, K.K.O., Swanson, D.R. et al (2019) Deep instability in the phylogenetic backbone of Heteroptera is only partly overcome by transcriptome-based phylogenomics. *Insect Systematics and Diversity*, 3, 1–14.
- Namyatova, A.A. & Cassis, G. (2019) First record of the subfamily Psallopinae (Heteroptera: Miridae) from Australia and discussion of its systematic position and diagnostic characters. *Austral Entomology*, 58, 156–170.
- Nguyen, L.T., Schmidt, H.A., von Haeseler, A. & Minh, B.Q. (2015) IQ-TREE: a fast and effective stochastic algorithm for estimating maximum-likelihood phylogenies. *Molecular Biology and Evolution*, 32, 268–274.
- Panizzi, A.R., Tiago, L. & Paula, L.M. (2021) Electronic monitoring of feeding behavior of phytophagous true bugs (Heteroptera). Cham: Springer Nature Switzerland AG.
- Paradis, E. & Schliep, K. (2019) ape 5.0: an environment for modern phylogenetics and evolutionary analyses in R. *Bioinformatics*, 35, 526–528.
- Percy, D.M., Page, R.D. & Cronk, Q.C. (2004) Plant-insect interactions: double-dating associated insect and plant lineages reveals asynchronous radiations. *Systematic Biology*, 53, 120–127.
- Petersen, M., Meusemann, K., Donath, A., Dowling, D., Liu, S., Peters, R.S. et al (2017) Orthograph: a versatile tool for mapping coding nucleotide sequences to clusters of orthologous genes. *BMC Bioinformatics*, 18, 111.
- Pluot-Sigwalt, D. & Moulet, P. (2020) Morphological types of spermatheca in Coreidae: bearing on intra-familial classification and tribal-groupings (Hemiptera: Heteroptera). *Zootaxa*, 4834(4), 451–501.
- Pluot-Sigwalt, D. & Lis, J.A. (2008) Morphology of the spermatheca in the Cydnidae (Hemiptera: Heteroptera): bearing of its diversity on classification and phylogeny. *European Journal of Entomology*, 105, 279–312.
- Popov, Y.A. (1971) Historical development of the infraorder Nepomorpha (Heteroptera). *Akademiya Nauk SSSR, Trudy Paleontologicheskogo Instituta*, 129, 1–228.
- Popov, Y.A. (1989) New fossil Hemiptera (Heteroptera and Coleorrhyncha) from the Mesozoic of Mongolia. *Neues Jahrbuch für Geologie und Paläontologie Monatshefte*, 3, 166–181.
- Popov, Y.A., Dolling, W.R. & Whalley, P.E.S. (1994) British Upper Triassic and Lower Jurassic Heteroptera and Coleorrhyncha (Insecta: Hemiptera). *Genus*, 5(4), 307–347.
- Popov, Y.A. & Herczek, A. (1992) The first Isometopinae from Baltic amber (Insecta: Heteroptera, Miridae). *Mitteilungen aus dem Geologisch-Paläontologischen Institut der Universität Hamburg*, 73, 241–258.
- Raup, D.M. (1979) Size of the Permo-Triassic bottleneck and its evolutionary implications. *Science*, 206, 217–218.
- Reineke, A., Karlovsky, P. & Zebitz, C.P.W. (1998) Preparation and purification of DNA from insects for AFLP analysis. *Insect Molecular Biology*, 7, 95–99.
- Reinhard, C.T., Planavsky, N.J., Olson, S.L., Lyons, T.W. & Erwin, D.H. (2016) Earth's oxygen cycle and the evolution of animal life. *Proceedings of the National Academy of Sciences of the United States of America*, 113, 8933–8938.
- Revell, L.J. (2012) Phytools: An R package for phylogenetic comparative biology (and other things). *Methods in Ecology and Evolution*, 3, 217–223.

- Roca-Cusachs, M., Schwertner, C.F., Kim, J., Eger, J., Grazia, J. & Jung, S. (2022) Opening Pandora's box: molecular phylogeny of the stink bugs (Hemiptera: Heteroptera: Pentatomidae) reveals great incongruence in the current classification. *Systematic Entomology*, 47, 36–51.
- Ronquist, F., Teslenko, M., van der Mark, P., Ayres, D.L., Darling, A., Höhna, S. et al (2012) MrBayes 3.2: efficient Bayesian phylogenetic inference and model choice across a large model space. *Systematic Biology*, 61, 539–542.
- Schaefer, C.W. (1975) Heteropteran trichobothria (Hemiptera: Heteroptera). *International Journal of Insect Morphology and Embryology*, 4, 193–264.
- Schaefer, C.W. & Panizzi, A.R. (2000) Heteroptera of economic importance. Boca Raton, FL: CRC Press.
- Schuh, R.T. (1974) The Orthotylinae and Phylinae (Hemiptera: Miridae) of South Africa with a phylogenetic analysis of the antimimetic tribes of the two subfamilies for the world. *Entomology Americana*, 47, 1–332.
- Schuh, R.T. (1976) Pretarsal structure in the Miridae (Hemiptera) with a cladistic analysis of relationships within the family. *American Museum Novitates*, 2601, 1–39.
- Schuh, R.T. & Štys, P. (1991) Phylogenetic analysis of cimicomorphan family relationships (Heteroptera). *Journal of the New York Entomological Society*, 99, 298–350.
- Schuh, R.T., Weirauch, C. & Wheeler, W.C. (2009) Phylogenetic relationships within the Cimicomorpha (Hemiptera: Heteroptera): a total-evidence analysis. *Systematic Entomology*, 34, 15–48.
- Schuh, R.T. & Weirauch, C. (2020) True bugs of the world (Hemiptera: Heteroptera): classification and natural history, 2nd edition. Rochdale, UK: Siri Scientific Press.
- Sharma, A., Khan, A.N., Subrahmanyam, S., Raman, A., Taylor, G.S. & Fletcher, M.J. (2014) Salivary proteins of plant-feeding hemipteroids—implication in phytophagy. *Bulletin of Entomological Research*, 104, 117–136.
- Shcherbakov, D.E. (2008) Insect recovery after the Permian/Triassic crisis. *Alavesia*, 2, 125–131.
- Shcherbakov, D.E. (2010) The earliest true bugs and aphids from the Middle Triassic of France (Hemiptera). *Russian Entomological Journal*, 19, 179–182.
- Slater, J.A. (1950) An investigation of the female genitalia as taxonomic characters in the Miridae (Hemiptera). *Iowa State College Journal of Science*, 25, 1–81.
- Slater, J.A. (1973) A contribution to the biology and taxonomy of Australian Thaumastocoridae with the description of a new species (Hemiptera: Heteroptera). *Australian Journal of Entomology*, 12, 151–156.
- Slater, J.A. (1976) Monocots and chinch bugs: a study of host plant relationships in the Lygaeid subfamily Blissinae (Hemiptera: Lygaeidae). *Biotropica*, 8(3), 143–165.
- Song, N., An, S.H., Yin, X.M., Zhao, T. & Wang, X.Y. (2016) Insufficient resolving power of mitogenome data in deciphering deep phylogeny of Holometabola. *Journal of Systematics and Evolution*, 54, 545–559.
- Štys, P. (1964) The morphology and relationship of the family Hyocephalidae (Heteroptera). *Acta Zoologica Academiae Scientiarum Hungaricae*, 10, 229–262.
- Štys, P. (1967) Monograph of Malcinae, with reconsideration of morphology and phylogeny of related groups (Heteroptera, Malcidae). *Acta Entomologica Musei Nationalis Pragae*, 37, 351–516.
- Sun, G., Dilcher, D.L., Zheng, S. & Zhou, Z. (1998) In search of the first flower: a Jurassic angiosperm, *Archaeofructus*, from northeast China. *Science*, 282, 1692–1695.
- Swanson, D.R. (2020) Misfit micrelytrines: revised identities for two extinct true bugs (Heteroptera). *Palaeoentomology*, 3, 546–551.
- Tennant, J.P., Mannion, P.D. & Upchurch, P. (2016) Sea level regulated tetrapod diversity dynamics through the Jurassic/Cretaceous interval. *Nature Communications*, 7, 12737.
- Theobald, N. (1937) Les insectes fossiles des terrains oligocènes de France. *Bulletin Mensuel (Mémoires) de la Société des Sciences de Nancy* 1, 1–473.
- Tian, X., Xie, Q., Li, M., Gao, C., Cui, Y., Li, X. et al (2011) Phylogeny of pentatomomorph bugs (Hemiptera-Heteroptera: Pentatomomorpha) based on six *Hox* gene fragments. *Zootaxa*, 2888, 57–68.
- Tian, Y., Zhu, W., Li, M., Xie, Q. & Bu, W. (2008) Influence of data conflict and molecular phylogeny of major clades in Cimicomorphan true bugs (Insecta: Hemiptera: Heteroptera). *Molecular Phylogenetics and Evolution*, 47, 581–597.
- Tillyard, R.J. (1926) Upper permian insects of new South Wales Part I. Introduction and the order Hemiptera. *Proceedings of the Linnean Society of New South Wales*, 51, 1–30.
- Tilmon, K.J. (2008) Specialisation, speciation, and radiation: the evolutionary biology of herbivorous insects. Berkeley, CA: University of California Press.
- Van Doesburg, P.H., Cassis, G. & Monteith, G.B. (2010) Discovery of a living fossil: a new xylastodorine species from New Caledonia (Heteroptera: Thaumastocoridae) and first record of the subfamily from the eastern Hemisphere. *Zoologische Mededelingen*, 84, 93–115.
- Wang, Y., Brožek, J. & Dai, W. (2020) Morphological disparity of the mouthparts in polyphagous species of Largidae (Heteroptera: Pentatomomorpha: Pyrrhocoroidea) reveals feeding specialization. *Insects*, 11(3), 145.
- Wang, Y.-H., Cui, Y., Rédei, D., Bañař, P., Xie, Q., Štys, P. et al (2016) Phylogenetic divergences of the true bugs (Insecta: Hemiptera: Heteroptera), with emphasis on the aquatic lineages: the last piece of the aquatic insect jigsaw originated in the Late Permian/Early Triassic. *Cladistics*, 32, 390–405.
- Wang, Y.-H., Moreira, F.F.F., Rédei, D., Chen, P.-P., Kuechler, S.M., Luo, J.-Y. et al (2021) Diversification of true water bugs revealed by transcriptome-based phylogenomics. *Systematic Entomology*, 46, 339–356.
- Wang, Y.-H., Wu, H.-Y., Rédei, D., Xie, Q., Chen, Y., Chen, P.-P. et al (2019) When did the ancestor of true bugs become stinky? Disentangling the phylogenomics of Hemiptera-Heteroptera. *Cladistics*, 35, 42–66.
- Ward, P.D. (2006) Out of thin air: Dinosaurs, birds, and Earth's ancient atmosphere. Washington, DC: Joseph Henry Press.
- Weirauch, C., Schuh, R.T., Cassis, G. & Wheeler, W.C. (2019) Revisiting habitat and lifestyle transitions in Heteroptera (Insecta: Hemiptera): insights from a combined morphological and molecular phylogeny. *Cladistics*, 35, 67–105.
- Wermelinger, B., Wyniger, D. & Forster, B. (2008) First records of an invasive bug in Europe: *Halyomorpha halys* Stål (Heteroptera: Pentatomidae), a new pest on woody ornamentals and fruit trees? *Mitteilungen der Schweizerischen Entomologischen Gesellschaft*, 81, 1–8.
- Wheeler, A.G. (2001) Biology of the plant bugs (Hemiptera: Miridae): pests, predators, opportunists. New York: Cornell University Press.
- Wheeler, W.C., Schuh, R.T. & Bang, R. (1993) Cladistic relationships among higher groups of Heteroptera: congruence between morphological and molecular data sets. *Entomologica Scandinavica*, 24, 121–137.
- Wu, K., Li, W., Feng, H. & Guo, Y. (2002) Seasonal abundance of the mirids, *Lygus lucorum* and *Adelphocoris* spp. (Hemiptera: Miridae) on Bt cotton in northern China. *Crop Protection*, 21, 997–1002.
- Wu, Y.-Z., Rédei, D., Eger, J. Jr, Wang, Y.-H., Wu, H.-Y., Carapezza, A. et al (2018) Phylogeny and the colourful history of jewel bugs (Insecta: Hemiptera: Scutelleridae). *Cladistics*, 34, 502–516.
- Xia, X.H. (2013) DAMBE5: a comprehensive software package for data analysis in molecular biology and evolution. *Molecular Biology and Evolution*, 30, 1720–1728.
- Xie, Q., Bu, W. & Zheng, L. (2005) The Bayesian phylogenetic analysis of the 18S rRNA sequences from the main lineages of Trichophora (Insecta: Heteroptera: Pentatomomorpha). *Molecular Phylogenetics and Evolution*, 34, 448–451.
- Xie, Y., Wu, G., Tang, J., Luo, R., Patterson, J., Liu, S. et al (2014) SOAPdenovo-Trans: de novo transcriptome assembly with short RNA-Seq reads. *Bioinformatics*, 30, 1660–1666.

- Yang, H., Li, T., Dang, K. & Bu, W. (2018) Compositional and mutational rate heterogeneity in mitochondrial genomes and its effect on the phylogenetic inferences of Cimicomorpha (Hemiptera: Heteroptera). *BMC Genomics*, 19, 264.
- Yang, L., Su, D., Chang, X., Foster, C.S.P., Sun, L., Huang, C.H. et al (2020) Phylogenomic insights into deep phylogeny of angiosperms based on broad nuclear gene sampling. *Plant Communications*, 1, 100027.
- Yang, Z. (2007) PAML 4: phylogenetic analysis by maximum likelihood. *Molecular Biology and Evolution*, 24, 1586–1591.
- Yao, Y.Z., Cai, W.Z. & Ren, D. (2007) The first fossil Cydnidae (Hemiptera: Pentatomoidea) from the Late Mesozoic of China. *Zootaxa*, 1388, 59–68.
- Ye, Z., Damgaard, J., Yang, H., Hebsgaard, M.B., Weir, T. & Bu, W. (2020) Phylogeny and diversification of the true water bugs (Insecta: Hemiptera: Heteroptera: Nepomorpha). *Cladistics*, 36, 72–87.
- Yu, S., Wang, Y., Rédei, D., Xie, Q. & Bu, W. (2013) Secondary structure models of 18s and 28s rRNAs of the true bugs based on complete rDNA sequences of *Eurydema maracandica* oshanin, 1871 (Heteroptera, Pentatomidae). *ZooKeys*, 319, 363–377.
- Yuan, M.L., Zhang, Q.L., Guo, Z.L., Wang, J. & Shen, Y.Y. (2015) Comparative mitogenomic analysis of the superfamily Pentatomoidea (Insecta: Hemiptera: Heteroptera) and phylogenetic implications. *BMC Genomics*, 16, 460.
- Zhang, J.F. (1989) Fossil insects from Shanwang, Shandong, China. Beijing: Science Press.
- Zhang, J., Weirauch, C., Zhang, G. & Forero, D. (2016) Molecular phylogeny of Harpactorinae and Bactrodinae uncovers complex evolution of sticky trap predation in assassin bugs (Heteroptera: Reduviidae). *Cladistics*, 32, 538–554.
- Zhang, L., Chen, F., Zhang, X., Li, Z., Zhao, Y., Lohaus, R. et al (2020) The water lily genome and the early evolution of flowering plants. *Nature*, 577, 79–84.

Supporting Information

Additional supporting information may be found online in the Supporting Information section at the end of the article.

Appendix S1. The details of fossil calibrations used in divergence time estimation.

Fig. S1. Phylogenetic tree of Terheteroptera based on PCGNT12RNA dataset including 150 taxon samples using maximum-likelihood analysis. The bootstrap values are shown around each node, and the bootstrap values < 50% are not shown.

Fig. S2. Phylogenetic tree of Terheteroptera based on PCGAARNA dataset including 150 taxon samples using maximum-likelihood analysis. The bootstrap values are shown around each node, and the bootstrap values < 50% are not shown.

Fig. S3. Phylogenetic tree of Terheteroptera based on PCGNT12RNA dataset including 150 taxon samples using Bayesian analysis. The Bayesian posterior probabilities values are shown around each node, and the Bayesian posterior probabilities values < 50% are not shown.

Fig. S4. Phylogenetic tree of Terheteroptera based on PCGAARNA dataset including 150 taxon samples using Bayesian analysis. The Bayesian posterior probabilities values are shown around each node, and the

Bayesian posterior probabilities values < 50% are not shown.

Fig. S5. Parsimony tree of Terheteroptera based on PCGNT12RNA dataset including 150 taxon samples.

Fig. S6. Parsimony tree of Terheteroptera based on PCGAARNA dataset including 150 taxon samples.

Fig. S7. Phylogenetic tree of Terheteroptera based on PCGNT12RNA dataset including 150 taxon samples using parsimony analysis with 1000 standard bootstrap resampling.

Fig. S8. Phylogenetic tree of Terheteroptera based on PCGAARNA dataset including 150 taxon samples using parsimony analysis with 1000 standard bootstrap resampling.

Fig. S9. Phylogenetic tree of Terheteroptera based on PCGNT12RNA dataset including 141 taxon samples using maximum-likelihood analysis. The bootstrap values are shown around each node, and the bootstrap values < 50% are not shown.

Fig. S10. Phylogenetic tree of Terheteroptera based on PCGAARNA dataset including 141 taxon samples using maximum-likelihood analysis. The bootstrap values are shown around each node, and the bootstrap values < 50% are not shown.

Fig. S11. Estimated divergence times of major terheteropteran lineages inferred from PCGNT12RNA maximum-likelihood tree and PCGNT12RNA dataset. Blue bars indicate 95% mean confidence intervals.

Fig. S12. Estimated divergence times of major terheteropteran lineages inferred from PCGAARNA maximum-likelihood tree and PCGAARNA dataset. Blue bars indicate 95% mean confidence intervals.

Fig. S13. Estimated divergence times of major terheteropteran lineages inferred from PCGNT12RNA Bayesian tree and PCGNT12RNA dataset. Blue bars indicate 95% mean confidence intervals.

Fig. S14. Estimated divergence times of major terheteropteran lineages inferred from PCGAARNA Bayesian tree and PCGAARNA dataset. Blue bars indicate 95% mean confidence intervals.

Fig. S15. Estimated divergence times of major terheteropteran lineages inferred from PCGNT12RNA parsimony tree and PCGNT12RNA dataset. Blue bars indicate 95% mean confidence intervals.

Fig. S16. Estimated divergence times of major terheteropteran lineages inferred from PCGAARNA parsimony tree and PCGAARNA dataset. Blue bars indicate 95% mean confidence intervals.

Fig. S17. The ancestral state reconstruction of feeding habit for major terheteropteran lineages inferred from PCGAARNA maximum-likelihood tree.

Fig. S18. The ancestral state reconstruction of feeding habit for major terheteropteran lineages inferred from PCGNT12RNA Bayesian tree.

Fig. S19. The ancestral state reconstruction of feeding habit for major terheteropteran lineages inferred from PCGAARNA Bayesian tree.

Fig. S20. The ancestral state reconstruction of feeding habit for major terheteropteran lineages inferred from PCGNT12RNA parsimony tree.

Fig. S21. The ancestral state reconstruction of feeding habit for major terheteropteran lineages inferred from PCGAARNA parsimony tree.

Table S1. Primer sequences of PCR amplification for mitogenome and nuclear rDNAs.

Table S2. The substitution saturation analyses.

Table S3. The partitioning schemes and models used for phylogenetic analyses.

Table S4. Feeding habit sources for ancestral state reconstruction.

Table S5. Estimation of divergence times (Ma) for major groups of Terheteroptera inferred from six topologies in this study.

Appendix dataset S1. The PCGAARNA matrix used for phylogenetic analyses.

Appendix dataset S2. The PCGNT12RNA matrix used for phylogenetic analyses.